JacketSE: An Offshore Wind Turbine Jacket Sizing Tool

Theory Manual and Sample Usage with Preliminary Validation

Rick Damiani
National Renewable Energy Laboratory

NREL is a national laboratory of the U.S. Department of Energy
Office of Energy Efficiency & Renewable Energy
Operated by the Alliance for Sustainable Energy, LLC

This report is available at no cost from the National Renewable Energy Laboratory (NREL) at www.nrel.gov/publications.

Technical Report
NREL/TP-5000-65417
February 2016

Contract No. DE-AC36-08GO28308

NREL
NATIONAL RENEWABLE ENERGY LABORATORY

JacketSE: An Offshore Wind Turbine Jacket Sizing Tool

Theory Manual and Sample Usage with Preliminary Validation

Rick Damiani
National Renewable Energy Laboratory

Prepared under Task No. WE11.5084

NREL is a national laboratory of the U.S. Department of Energy
Office of Energy Efficiency & Renewable Energy
Operated by the Alliance for Sustainable Energy, LLC

This report is available at no cost from the National Renewable Energy Laboratory (NREL) at www.nrel.gov/publications.

National Renewable Energy Laboratory
15013 Denver West Parkway
Golden, CO 80401
303-275-3000 • www.nrel.gov

Technical Report
NREL/TP-5000-65417
February 2016

Contract No. DE-AC36-08GO28308

This report is available at no cost from the National Renewable Energy Laboratory (NREL) at www.nrel.gov/publications.

Available electronically at SciTech Connect http:/www.osti.gov/scitech

Available for a processing fee to U.S. Department of Energy and its contractors, in paper, from:

U.S. Department of Energy
Office of Scientific and Technical Information
P.O. Box 62
Oak Ridge, TN 37831-0062
OSTI http://www.osti.gov
Phone: 865.576.8401
Fax: 865.576.5728
Email: reports@osti.gov

Available for sale to the public, in paper, from:

U.S. Department of Commerce
National Technical Information Service
5301 Shawnee Road
Alexandria, VA 22312
NTIS http://www.ntis.gov
Phone: 800.553.6847 or 703.605.6000
Fax: 703.605.6900
Email: orders@ntis.gov

Cover Photos by Dennis Schroeder: (left to right) NREL 26173, NREL 18302, NREL 19758, NREL 29642, NREL 19795.

NREL prints on paper that contains recycled content.

Executive Summary

This manual summarizes the theory and preliminary verifications of the JacketSE module, which is an offshore jacket sizing tool that is part of the Wind-Plant Integrated System Design & Engineering Model toolbox. JacketSE is based on a finite-element formulation and on user-prescribed inputs and design standards' criteria (constraints). The physics are highly simplified, with a primary focus on satisfying ultimate limit states and modal performance requirements. Preliminary validation work included comparing industry data and verification against ANSYS, a commercial finite-element analysis package. The results are encouraging, and future improvements to the code are recommended in this manual.

Acknowledgments

This work was supported by the U.S. Department of Energy under Contract No. DE-AC36-08GO28308 with the National Renewable Energy Laboratory. Funding for the work was provided by the DOE Office of Energy Efficiency and Renewable Energy, Wind and Water Power Technologies Office.

Table of Contents

List of Figures

List of Tables

List of Acronyms and Symbols

Acronyms

t	Wall thickness
AHSE	Aero-hydro-servo-elastic
BOS	Balance-of-system
CAE	Computer-aided engineering
CapEx	Capital expenditure
DLC	Design load case
FAST v8	National Renewable Energy Laboratory (NREL)'s aero-elastic tool
FEA	Finite-element analysis
FLS	Fatigue limit state
LCOE	Levelized cost of energy
LRFD	Load Resistance Factor Design
MSL	Mean sea level

NOAA	National Oceanic and Atmospheric Administration
NREL	National Renewable Energy Laboratory
O&G	Oil and gas
O&M	Operation and maintenance
OD	Outer diameter
OEM	Original equipment manufacturer
OR	Outer radius
OWT	Offshore wind turbine
PSF	Partial safety factor
RNA	Rotor nacelle assembly
SACS	A commercial package by Bentley for the analysis of offshore fixed-bottom structures
SLS	Serviceability limit state
SSt	Support structure
TP	Transition piece
ULS	Ultimate limit state
WISDEM	Wind-Plant Integrated System Design & Engineering Model

Symbols

$2D$	Two-dimensional
AB	Distance between the first two leg joints at the bottom bay
A_1	First point of segment $\overline{A_1A_2}$
A_2	Second point of segment $\overline{A_1A_2}$
A_p	Surface area of the pile tip
A_s	Side surface area of the pile
A_{brc}	Brace cross-sectional area
A_{jnt}	Factor in the calculation of Q_{fc} per API 2014
A_{leg}	Leg cross-sectional area
A_{mid}	Area inscribed by the midthickness line
A	Member cross-sectional area
B_1	First point of segment $\overline{B_1B_2}$
B_2	Second point of segment $\overline{B_1B_2}$
CM	Center of mass
CP_{fg}	Flag indicating whether (True) or not (False) the legs are considered clamped at the seabed
C_τ	Factor in the expression of $\tau_{z\theta,Rcr}$
C_θ	Factor in the expression of $\sigma_{\theta,Rcr}$
C_c	Reduction factor in the calculations of the axial stress allowables for members under compression per API 2014
C_m	Reduction factor in the calculations of the utilization for members under compression and bending per API 2014
C_z	Factor in the expression of $\sigma_{z,Rcr}$
$C_{\theta,s}$	Factor in the expression of $\sigma_{\theta,Rcr}$
C_{fxe}	Reduction factor in the calculation of the elastic buckling stress per API 2014, which is normally equal to 0.3

C_{l2g}	Transformation matrix from local to global coordinate system
DTR_b	Tower-base Diameter to thickness ratio (DTR)
DTR_t	Tower-top DTR
DTR	Diameter to thickness ratio
D_1	Bottom Outer diameter (OD) of a tapered shell member
D_2	Top OD of a tapered shell member
D_b	Tower-base OD
D_p	Pile outer diameter
D_t	Tower-top OD
D_{TPbrc}	TP cross-brace OD
D_{brc1}	D_{brc} for brace 1 at the k-joint
D_{brc2}	D_{brc} for brace 2 at the k-joint
D_{brc}	Brace outer diameter
D_{gir}	TP girder OD
D_{leg}	Leg outer diameter
D_{lt}	Leg top OD
D_{mbrc}	Mud-brace outer diameter
D_{sh}	Shell OD
D_{stmp}	TP stump OD
D_{strt}	TP strut OD
D_{tbrc}	Top-brace outer diameter
D_{xbrc}	X-brace outer diameter
D	Generic member OD
E_p	Pile Young's modulus
E_s	Soil modulus or modulus of subgrade reaction ($\mathrm{N\,m^{-2}}$)
E	Young's modulus
F_a	Allowable axial compressive stress
F_b	Allowable bending stress
F_d	Generic, design (factored) load within the Load Resistance Factor Design (LRFD) approach
$F_e\prime$	Euler stress divided by a safety factor per AISC 1989
F_k	Generic, characteristic load within the LRFD approach
$F_{p,x}$	Reaction force along x at pile head
$F_{p,y}$	Reaction force along y at pile head
$F_{p,z}$	Reaction force along z at pile head
$F_{x_{RNA}}$	Force from the RNA along the x-axis
$F_{y_{RNA}}$	Force from the RNA along the y-axis
$F_{z_{RNA}}$	Aerodynamic force from the RNA along the z axis
G_f	Gust factor
G_p	Pile material shear modulus
G_s	Initial soil shear modulus at depth of interest
$G_{s,c}$	Soil shear modulus at torsional critical depth
G	Shear modulus
IP	In-plane
I_{xx}	Mass second moment of inertia about the local x axis
I_{xy}	Mass cross-moment of inertia about the x–y axes
I_{xz}	Mass cross-moment of inertia about the x–z axes
I_{yy}	Mass second moment of inertia about the local y axis
I_{yz}	Mass cross-moment of inertia about the y–z axes
I_{zz}	Mass second moment of inertia about the local z axis
$J_{xx,p}$	Pile cross-sectional, second area moment of inertia
J_{xx}	Member cross-sectional, second area-moment of inertia

KLR_{brc}	Brace KLR
KLR	Buckling parameter $k_{buck} l_{tube} / r_{gyr}$
K_g	Stiffness matrix referred to global coordinate system
K_l	Stiffness matrix referred to local coordinate system
K_p	Modulus ratio used in Pender's method
K_{API}	Coefficient of lateral earth pressure
L_a	Pile active length
L_c	Pile critical embedment length for torsion response
L_p	Pile embedment length
L	Generic member length
M_a	Allowable capacity for brace bending load
M_d	Design (factored) bending moment load at the station of interest
M_j	Brace bending load at the joint
M_p	Bending moment load resistance at the tower station of interest
M_x	Component of the bending moment along the x-axis at the station of interest
M_y	Component of the bending moment load along the y-axis at the station of interest
M_z	Torsion moment load along the z-axis at the station of interest
$M_{c,IP}$	Chord IP bending load at the joint
$M_{jnt,x}$	Local x component of $\mathbf{M_{jnt}}$
$M_{jnt,y}$	Local y component of $\mathbf{M_{jnt}}$
$M_{jnt,z}$	Local z component of $\mathbf{M_{jnt}}$
M_{mod}	Method to be used for dyanmic eigenvalue: 1=Subspace-Jacobi iteration; 2= Stodola (matrix iteration) method Gavin 2010
$M_{p,x}$	Reaction moment along x at pile head
$M_{p,y}$	Reaction moment along y at pile head
$M_{p,z}$	Reaction moment along z at pile head
M_{pc}	Plastic moment capacity of the chord at the joint
$M_{x_{RNA}}$	RNA aerodynamic moment along the x-axis
$M_{y_{RNA}}$	RNA aerodynamic moment along the y-axis
$M_{z_{RNA}}$	RNA aerodynamic moment along the z-axis
N_d	Design (factored) normal load at the tower station of interest
N_e	Elastic buckling resistance
N_p	Normal (axial) load resistance at the tower station of interest
N_q	Dimensionless bearing capacity factor
OP	Out-of-plane
$P-\Delta$	P-Δ effect
PP_{fg}	Flag indicating whether (True) or not (False) the piles are considered 'plugged'
P_a	Allowable capacity for brace axial load
P_c	Chord axial load at the joint
P_j	Brace axial load at the joint
P_{yc}	Yield capacity of the chord at the joint
$Q-z$	Nonlinear spring treatment of soil-pile end-bearing, axial stiffness
Q_d	Ultimate bearing capacity of pile
Q_f	Skin friction resistance
Q_g	Gap factor at a joint per API 2014
Q_p	End bearing resistance
Q_{beta}	Geometric factor at a joint per API 2014
Q_{fc}	Chord load factor per API 2014
Q_{ub}	Strength factor per API 2014
Q	Meridional compression fabrication quality parameter European Committee for Standardisation 1993
$R(f_d)$	Probability distribution of the generic, design (factored) material resistance within the LRFD approach

R_{dx}	Method for matrix condensation: 0= none; 1= static; 2=Guyan; 3=dynamic Gavin 2010
$S(F_d)$	Probability distribution of the generic, design (factored) load within the Load Resistance Factor Design approach
TP_{lvl}	Level of automatic build for the TP
T_d	Design (factored) shear load at the station of interest
T_w	Wave spectral period
T_x	Component of the shear load along the x-axis at the station of interest
T_y	Component of the shear load along the y-axis at the station of interest
T_{mr}	Relative stiffness factor from Matlock and Reese 1960
VP_{fg}	Flag indicating whether the piles are vertical (True) or battered (False)
W_p	Cross-sectional bending modulus
$[\mathbf{C}_\phi]$	Matrix describing the transformation of coordinate systems from $\mathscr{F}\mathscr{F}_1$ to $\mathscr{F}\mathscr{F}_2$ via a rotation about the local x
$[\mathbf{C}_{\psi,\theta}]$	Matrix describing the transformation of coordinate systems from $\mathscr{F}\mathscr{F}_0$ to $\mathscr{F}\mathscr{F}_1$ via a rotation θ_{el} about the global y and a rotation ψ_{el} about global z
$[\mathbf{C_{el}}]$	Matrix identifying the local element coordinate system, i.e., the transformation from $\mathscr{F}\mathscr{F}_0$ to $\mathscr{F}\mathscr{F}_2$, with local x along the member axis and local y, z along the cross-section principal axes of inertia
$[\mathbf{C_{jnt}}]$	Direction cosine matrix identifying the joint plane, with x, y in the joint plane and z normal to it
$\hat{G}_p$	Equivalent shear modulus used for piles
$\hat{i}$	Unit vector along the x-axis
$\hat{j}$	Unit vector along the y-axis
$\mathbf{CM_{off}}$	Distance vector from the tower-top flange to the *CM* of the RNA
$\mathbf{C_{el,x}}$	First row of $[\mathbf{C_{el}}]$
$\mathbf{C_{el,y}}$	Second row of $[\mathbf{C_{el}}]$
$\mathbf{C_{el,z}}$	Third row of $[\mathbf{C_{el}}]$
$\mathbf{C_{jnt,x}}$	First row of $[\mathbf{C_{jnt}}]$
$\mathbf{C_{jnt,y}}$	Second row of $[\mathbf{C_{jnt}}]$
$\mathbf{C_{jnt,z}}$	Third row of $[\mathbf{C_{jnt}}]$
$\mathbf{D_{stem}}$	Array of TP central shell ODs (one per shell member)
$\mathbf{F_{aero}}$	Force vector originating at the rotor
$\mathbf{M_{IP}}$	*IP* component of the bending moment vector for the generic member at the joint of interest
$\mathbf{M_{OP}}$	*OP* component of the bending moment vector for the generic member at the joint of interest
$\mathbf{M_{aero}}$	Moment vector originating at the rotor
$\mathbf{M_{jnt}}$	Bending moment vector for the generic member at the joint of interest
$\mathbf{TP_{mas}}$	TP lumped mass, including mass, mass tensor (I_{xx}–I_{zz}) and *CM* offset from the center of the deck
$\mathbf{U_w}$	Vectorial sum of the wave and current velocity
$\mathbf{U_{hub}}$	Wind velocity at hub height
$\mathbf{U}$	Wind velocity vector
$\boldsymbol{\delta}_{\mathbf{thoff}}$	Distance vector from the tower-top flange to the hub center
$\hat{\mathbf{i}}_{\mathbf{brc}}$	Unit vector identifying the x-brace longitudinal axis
$\hat{\mathbf{i}}_{\mathbf{ch}}$	Unit vector identifying the chord longitudinal axis
$\mathbf{f_a}$	Force per unit length caused by wind aerodynamic drag
$\mathbf{f_w}$	Force per unit length as a result of wave and current kinematics
$\mathbf{h_{bys}}$	Array containing the bay heights
$\mathbf{h_{stem}}$	Array of TP central shell lengths (one per shell member)
$\mathbf{t_{stem}}$	TP central shell Wall thicknesses (t's) (one per shell member)
$\mathbf{u_c}$	Current velocity
$\mathbf{u_w}$	Wave velocity
$\mathscr{F}\mathscr{F}_0$	Global coordinate system
$\mathscr{F}\mathscr{F}_1$	Auxiliary coordinate system
$\mathscr{F}\mathscr{F}_2$	Local coordinate system

$\mathscr{L}$	Ratio of the pile length to its diameter
$\mathscr{R}$	Ratio of pile Young's modulus to soil modulus at pile tiplength to diameter
ν_s	Soil Poisson's ratio
$\overline{A_1A_2}$	Vector connecting A_1 to A_2
$\overline{B_1B_2}$	Vector connecting B_1 to B_2
$\underline{AB}_c$	Vector resulting from the cross product of $\overline{A_1A_2}$ and $\overline{B_1B_2}$
$\underline{A}_0$	Set of coordinates for intersection between $\overline{A_1A_2}$ and $\overline{B_1B_2}$
$\underline{A}_1$	Set of coordinates for first point of segment $\overline{A_1A_2}$
$\vec{g}$	Inertial frame acceleration for FRAME3DD
b	Two-dimensional batter, i.e., the vertical-to-horizontal ratio of the jacket-leg slope on a $2D$ projection
c_1	Factor in the calculation of Q_{fc} per API 2014
c_2	Factor in the calculation of Q_{fc} per API 2014
c_3	Factor in the calculation of Q_{fc} per API 2014
c_d	Drag coefficient (wind or water)
c_m	Added mass coefficient
c_u	Undrained shear strength
$c_{d,aj}$	Air drag coefficient jacket
$c_{d,at}$	Air drag coefficient tower
$c_{d,wj}$	Water drag coefficient jacket
d_w	Water depth
d_{jb}	Brace OD in a joint verification (also t_{xbrc})
d_{jc}	Chord OD at a joint (also D_{leg})
dck_w	Deck-side length
f_0	First natural frequency in Hz
f_d	Generic, design (factored) resistance within the LRFD approach
f_k	Generic, characteristic material resistance within the LRFD approach
f_y	Characteristic yield strength
$f_{\theta\theta}$	Flexibility matrix coefficient at pile head, representing the rotation about y associated with a unit moment along y
$f_{\theta x}$	Flexibility matrix coefficient at pile head, representing the displacement about y associated with a unit moment along y
f_{max}	Upper bound for th eshaft friction value for cohesionless soils
f_{stem}	Ratio between the TP central-shell wall thickness and t_b
$f_{x\theta}$	Flexibility matrix coefficient at pile head, representing the lateral displacement along x associated with a unit moment along y
f_{xc}	Inelastic local buckling stress
f_{xe}	Elastic local buckling stress
f_{xx}	Flexibility matrix coefficient at pile head, representing the lateral displacement along x associated with a unit force along x
f_{y2}	Allowable used in local buckling axial stress determination per API 2014
f_{yb}	Brace allowable stress used in joint verification
f_{yc}	Chord allowable stress used in joint verification
f	Skin friction
g_p	Gap between two braces at a k-joint per API 2014
gm_{fg}	Geometric stiffness effect flag for FRAME3DD
g	Gravity acceleration
h_c	Height of a tapered shell member
h_w	Wave height, (peak-to-peak distance)
h_{2f}	Fraction of tower length at constant cross section
$h_{b,1}$	Height of the bottom bay
$h_{b,i}$	Height of the i-th bay, counting from the bottom bay up

h_{jckt}	Height of the jacket available to the bays
h_{lb}	Distance from the leg-toe to the first joint with an x-brace
h_{stmp}	TP stump length
h_{twrb}	Tower buckling effective length, shortest distance between flanges
h_{twr}	Tower length
$hydc$	Hydrostatic constant
i	Generic index
k_τ	Exponent factor for the shear stress ratio, in the local buckling utilization calculation
k_θ	Exponent factor for the hoop stress ratio, in the local buckling utilization calculation
k_i	Interaction (axial-hoop stresses) factor in the local buckling utilization calculation
k_s	Coefficient of subgrade reaction
k_w	Dynamic pressure factor to calculate hoop stresses function of cylinder dimensions and external pressure buckling factor per European Committee for Standardisation (1993)
k_z	Exponent factor for the axial stress ratio, in the local buckling utilization calculation
$k_{\theta_x y}$	Stiffness matrix coefficient, representing the moment about x associated with a unit displacement along y
$k_{\theta_x \theta_x}$	Stiffness matrix coefficient, representing the moment about x associated with a unit rotation about x
$k_{\theta_y x}$	Stiffness matrix coefficient, representing the moment about y associated with a unit displacement along x
$k_{\theta_y \theta_y}$	Stiffness matrix coefficient, representing the moment about y associated with a unit rotation about y
$k_{\theta_z \theta_z}$	Stiffness matrix coefficient, representing the torsional moment about z associated with a unit rotation about z
k_{buck}	Buckling parameter or effective length factor
$k_{x\theta_y}$	Stiffness matrix coefficient, representing the lateral force along x associated with a unit rotation about y
k_{xx}	Stiffness matrix coefficient, representing the lateral force along x associated with a unit displacement along x
$k_{y\theta_x}$	Stiffness matrix coefficient, representing the lateral force along y associated with a unit rotation about x
k_{yy}	Stiffness matrix coefficient, representing the lateral force along y associated with a unit displacement along y
k_{zz}	Stiffness matrix coefficient, representing the axial force along z associated with a unit displacement along z
l_m	Method for mass modeling: 0= consistent mass matrix method; 1=lumped mass matrix method Gavin 2010
$l_{b,1}$	Length of the bottom x-brace
l_{tube}	Tube object unsupported length
m_{RNA}	RNA mass
mat	Object class defining material properties
n_A	Auxiliary quantity used in the calculation of the intersection between $\overline{A_1 A_2}$ and $\overline{B_1 B_2}$ segments
n_{bays}	Number of bays
$n_{div,TPbrc}$	Number of elements in each of the TP cross-brace members
$n_{div,gir}$	Number of elements in each of the TP girder members
$n_{div,leg}$	Number of elements in the leg member
$n_{div,mud}$	Number of elements in the mud-brace member
$n_{div,pile}$	Number of elements in the pile member
$n_{div,stmp}$	Number of elements in each of the TP stumps
$n_{div,strt}$	Number of elements in each of the TP struts
$n_{div,tbrc}$	Number of elements in the top-brace member
$n_{div,twr}$	Number of elements in each of the two tower segments
$n_{div,xbrc}$	Number of elements in the x-brace member
n_{div}	Number of elements in the member under consideration
n_{legs}	Number of legs in the substructure (equal to the number of piles)
n_{mod}	Number of eigenmodes to be calculated by FRAME3DD
n_{stem}	Number of TP shell members

$p-y$	Nonlinear spring treatment of soil-pile lateral stiffness
p'_o	Overburden pressure at the depth of interest
q_a	Soil allowable bearing-capacity
q_p	Unit end bearing capacity
q_{max}	Maximum wind dynamic pressure
$q_{p,max}$	Upper bound for the unit end bearing capacity
r_{eq}	Equivalent untapered Outer radius (OR) of a tapered shell member
r_{gyr}	Cross-section radius of gyration
rig_{flg}	Flag selecting how to treat the rigid connection at tower-top with the RNA
rtr	Ratio of r_{eq} to t_{eq}
s_k	Buckling length factor, set equal to 2 for the tower
sh_{fg}	Shear deformation effect flag for FRAME3DD
$t-z$	Nonlinear spring treatment of soil-pile axial stiffness
t_1	Bottom t of a tapered shell member
t_2	Top t of a tapered shell member
t_b	Tower-base t
t_p	Pile wall thickness
t_t	Time variable
t_{TPbrc}	TP cross-brace t
t_{eq}	Equivalent untapered t of a tapered shell member
t_{gir}	TP girder t
t_{jb}	Brace t in a joint verification (also t_{xbrc})
t_{jc}	Chord thickness in a joint verification (also t_{leg})
t_{leg}	Leg wall thickness
t_{mbrc}	Mud-brace wall thickness
t_{sh}	Shell t
t_{stmp}	TP stump t
t_{strt}	TP strut t
t_{tbrc}	Top-brace wall thickness
t_{xbrc}	X-brace wall thickness
$tube$	Tube object class
$tube$	Number of elements per member in each leg
$u_{p,x}$	Pile head displacement along x
$u_{p,y}$	Pile head displacement along y
$u_{p,z}$	Pile head displacement along z
w_b	Width of the jacket base (length of one side) at the seabed
$w_{b,1}$	Horizontal distance between the leg-to-brace joints at bay 1 (bottom bay), i.e., bay-1 bottom width
$w_{b,2}$	Second bay width
$w_{b,i}$	Width of i-th bay (bays counted from bottom up, $1..n_{bays}$
wdr	Allowance for weldments as a function of member diameter
x_{leg}	Generic leg joint or node coordinate along x
x	Global (or local) x-axis
y_{leg}	Generic leg joint or node coordinate along y
y	Global (or local) y-axis
z_d	Depth below the seabed
z_w	Distance from the sea surface, positive upwards
z_{RNA}	Z coordinate of the RNA CM
z_{cmoff}	Distance from the tower-top flange to the RNA CM along z
z_{dbot}	Deck underside elevation Mean sea level (MSL)
z_{hub}	Hub height above MSL
z_{lb}	Elevation of the leg-toe above the seabed

z_{leg}	Generic leg joint or node coordinate along z
z_{tb}	Elevation MSL of tower-base
z_{thoff}	Distance from the tower-top flange to the hub center along z
z	Global (or local) z-axis
z	Altitude above MSL
ANSYS	Ansys commercial Finite-element analysis (FEA) package
FRAME3DD	Open-source FEA package, Gavin 2010
JacketSE	Offshore jacket sizing tool, part of Wind-Plant Integrated System Design & Engineering Model (WISDEM)
k-joint	Joint at the intersection between leg and x-braces
mud-brace	Mud-brace
pyFrame3DD	Python wrapper for FRAME3DD
Quattropod®	Patented jacket configuration by OWEC Tower AS
TowerSE	Tower and monopile sizing tool, part of WISDEM
x-brace	X-brace
x-joint	Joint at the intersection betwee x-braces

Greek Symbols

Δ_n	Factor accounting for member slenderness in the global buckling utilization calculation
Δ_z	Step size for internal force calculations along the member axis for FRAME3DD
Δw_k	Characteristic imperfection amplitude European Committee for Standardisation 1993
Δz_{mx}	Maximum FEA element length for the tower elements
Φ	Factor used in the flexural buckling reduction factor calculation
α_b	Imperfection factor used in the buckling calculation, set equal to 0.21 in JacketSE
α_s	Factor used in cohesive soils to calculate shaft friction
$\alpha_{bat,2D}$	Two-dimensional batter angle
$\alpha_{bat,3D}$	Three-dimensional batter angle
α_{bl1}	Angle between brace 1 and leg at the k-joint
α_{bl2}	Angle between brace 2 and leg at the k-joint
α_{imp}	Elastic imperfection reduction factor from European Committee for Standardisation 1993
α	Wind power law exponent
$\bar{\lambda}$	Reduced slenderness (see Germanischer Lloyd 2005)
β_c	Cone angle for the typical tapered shell element
β_j	Ratio of brace diameter to chord diameter
β_m	Bending moment coefficient in the global buckling utilization calculation
β_p	Plastic range factor in the shell buckling verification
β_{2D}	Brace-to-leg angle as measured on a vertical projection
β_{3D}	Actual brace-to-leg angle
χ_θ	Buckling reduction factor for hoop strength in the shell buckling verification
χ_z	Buckling reduction factor for axial strength in the shell buckling verification

χ	Generic buckling reduction factor in the shell buckling verification
δ_f	Dynamic amplification factor
δ_s	Soil-to-steel friction angle
$\delta_{el,x}$	Component along global x of $\boldsymbol{\delta_{el}}$
$\delta_{el,y}$	Component along global y of $\boldsymbol{\delta_{el}}$
$\delta_{el,z}$	Component along global z of $\boldsymbol{\delta_{el}}$
δ_{shf}	Frequency shift factor for rigid-body modes Gavin 2010
η	Interaction exponent in the shell buckling verification
γ_b	Safety factor used in buckling verification, usually set equal to 1.1 (Germanischer Lloyd 2005)
γ_c	Ratio of d_{jc} to twice the t_{jc} at the joint
γ_f	Generic load PSF
γ_m	Material PSF
γ_n	Consequence of failure PSF
γ_s	Soil unit weight
γ_{fa}	Aerodynamic load PSF
γ_{fg}	Gravitational load PSF
γ_{fw}	Hydrodynamic load PSF
γ_{in}	Angle described by the horizontal projection of one side of the jacket base and a line connecting the center of the polygon at the base and one end of that side
γ_{j1}	Brace load PSF in a joint verification, which is normally set at 1.6
γ_{j2}	Chord PSF in a joint verification, which is normally set equal to 1.2
$\hat{\lambda}_0$	Squash limit for reduced slenderness
$\hat{\lambda}_p$	Plastic limit for the reduced slenderness
$\hat{\lambda}$	Reduced slenderness
κ_w	Wave number
κ	Reduction factor in the global buckling utilization calculation
$\boldsymbol{\delta_{el}}$	Distance vector between two adjacent nodes of a FEA element
ν	Poisson's ratio
ω_b	Dimensionless length parameter for shell buckling calculations
ω_w	Wave frequency
ϕ_s	Soil friction angle
ϕ_{el}	Eulerian rotational angle about the local x
ϕ_{rot}	Rotation angle about the local x-axis
ψ_s	Factor used in cohensionless soils for the determination of the pile shaft friction
ψ_{el}	Rotational angle about the global z (per FRAME3DD's convention)
ψ_{rot}	Rotation angle about the local z axis
ψ	Rotor yaw angle about global z
ρ_a	Air density
ρ_w	Sea water density
ρ	Material density
σ_a	Normal stress caused by axial force
σ_b	Normal stress caused by total bending moment
$\sigma_{\theta,Ed}$	Hoop design (factored) stress
$\sigma_{\theta,Rcr}$	Critical buckling hoop stress
$\sigma_{\theta,Rd}$	Hoop buckling strength
$\sigma_{b,x}$	Normal stress caused by bending about local x
$\sigma_{b,y}$	Normal stress caused by bending about local y
σ_{vm}	von-Mises stress
$\sigma_{z,Ed}$	Axial (meridional) design (factored) stress
$\sigma_{z,Rcr}$	Critical buckling axial stress
$\sigma_{z,Rd}$	Axial (meridional) buckling strength

$\tau_{z\theta,Ed}$	Shear design (factored) stress
$\tau_{z\theta,Rcr}$	Critical buckling shear stress
$\tau_{z\theta,Rd}$	Shear buckling strength
θ_j	Smaller angle described by the brace's and chord's axes at the joint
θ_{el}	Rotational angle about the global y (per FRAME3DD's convention)
$\theta_{p,x}$	Pile head rotation along x
$\theta_{p,y}$	Pile head rotation along y
$\theta_{p,z}$	Pile head rotation along z
ζ	Dummy coordinate along the z-axis

1 Introduction

The European Wind Energy Association (EWEA 2015) reports that in Europe, by the end of 2014, 78.8% of the installed substructures were monopiles, with lattice structures such as jackets accounting for 4.7%, and the remainder were gravity foundations, tripods, and tripiles. Although monopiles are still considered as preferred substructures because of their ease of fabrication and installation, it is unclear whether this trend will apply in the United States, where challenging bathymetry, soil conditions, and sea states may make monopiles economically less attractive. The first U.S. offshore wind installation (Deepwater Wind offshore of Rhode Island) is making use of jackets.

Several studies (e.g., Musial, Butterfield, and Ram 2006; De Vries et al. 2011), have shown that monopiles, likely the most readily available solution for shallow waters, are progressively unfeasible as projects are sited in deeper water and use larger turbine sizes (6 MW and above). Monopiles require large structural mass to guarantee system modal performance, and can become expensive and difficult to manufacture and install. In contrast, a lattice substructure can deliver needed structural stiffness by efficiently increasing its footprint.

Typical design practice for an offshore wind turbine (OWT) assumes a fixed turbine (and, in most cases, turbine-tower) configuration and requires multiple iterations to arrive at a final layout for the support structure (i.e., the substructure, foundation, and tower). The substructure's (and foundation's) design is generally carried out by a different engineering entity, requiring, at each iteration, an exchange of loads and stiffness data with the turbine original equipment manufacturers (OEMs). The geometry of the substructure is determined by satisfying the serviceability limit state (SLS), fatigue limit state (FLS), and ultimate limit state (ULS) under combined turbine loads and hydrodynamic loads. A change in the substructure design directly impacts the system dynamics and structural integrity, thus it must be followed by a reverification of the turbine loads' envelope. As a result of this sequential approach to the support structure design, aspects of the fully-coupled dynamics may be missed along with the risk of achieving suboptimal solutions. Because of the lack of fully coupled analyses, important trade-offs in the design of the subsystems are not fully considered, and the resulting system cost can be higher than that of the optimal solution.

Suboptimal designs of the support structure are particularly detrimental because they directly influence capital expenditure (CapEx), balance-of-system (BOS) costs, and the operation and maintenance (O&M) costs. According to Mone et al. 2015, the substructure and foundation are responsible for 14% of the total offshore wind plant levelized cost of energy (LCOE), and the largest uncertainty in LCOE is attributed to its sensitivity to CapEx, which is dominated by the support structure.

Capturing these cost relationships with respect to main environmental design drivers (Damiani et al. 2016) is a formidable challenge that the wind industry faces in the quest for lower LCOE and improved reliability and performance. An integrated design of the turbine and support structure may have the potential to significantly lower the overall system cost. Adding the control system in the loop would further compound the opportunities for loads, material mass, and cost reduction. To enable this system-level optimization, physics-based models of all major system components are required to explicitly capture the trade-offs between their designs.

The National Renewable Energy Laboratory (NREL) developed the wind energy systems engineering toolbox WISDEM (NREL 2015) to address some of the above issues. WISDEM integrates a variety of models for the entire wind energy system, including turbine and plant equipment, O&M, and cost modeling (Dykes et al. 2011). Although sophisticated load simulations conducted through aero-hydro-servo-elastic tools can account for all ULS and FLS design load cases (DLCs), and for an accurate representation of all physical couplings between component dynamics, these simulations are computationally expensive and time intensive. Simplified tools can guide the preliminary design of components and of the overall system towards a configuration that minimizes the LCOE through multidisciplinary optimization.

Within WISDEM, NREL developed physics-based models for the tower and monopile substructure (TowerSE). They are relatively simple and mostly based on modal analysis and buckling verification of the main segments of a steel tubular tower; however, these models do not directly port over to the analysis of a lattice structure. JacketSE was developed to allow for the analysis of OWTs using jacket-based support structures.

JacketSE is based on an open-source finite-element analysis (FEA) package (FRAME3DD) that can handle Timoshenko beam elements arranged in a beam-frame configuration. A set of structural code checks based on API (2014) is used to verify members and joints of the substructure, whereas the tower portion of the support structure uses the same set as in TowerSE. Simplified hydrodynamics also is in common with the TowerSE module. Examples of results and preliminary verification of the software can be found in Damiani and Song (2013) and Damiani et al. (2016), but more validation remains necessary.

The most common jacket configuration is the Quattropod®[1], or four-legged lattice, with x-bracing between the legs forming multiple bays (3–5 for water depths of 20-50 m), with a transition piece (TP) starting at deck-height and terminating at the tower flange, and with piles secured via special plate-sleeves at the bottom of the legs. As a result, this is the reference configuration modeled by JacketSE (depicted in Figure 1).

The constraints used on the jacket design follow industry experience but are still sufficiently relaxed to allow for tighter optimizations. To arrive at more realistic estimates and detailed designs, standard ODs and *DTR*s for the lattice members and piles should be employed. More recently proposed solutions call for three-legged multimember substructures, as they save mass and construction labor costs. Yet, these configurations require other expedients to generate the necessary stiffness, for example, by raking the legs as in the inward battered guided structure by Keystone Engineering Inc. (BVG Associates 2012). These more complex layouts are outside the scope of the work presented here and will be addressed in future software versions. Nevertheless, a basic three-legged, prepiled, battered jacket can still be modeled by JacketSE.

JacketSE can be used for either stand-alone support-structure analysis and design or as part of a larger wind turbine or wind plant study. In stand-alone mode, JacketSE aids the designer in the search for an optimal preliminary configuration of the substructure and tower, and for given environmental loading conditions, turbine dynamic loading, modal performance targets, and standards design criteria. The optimization criteria (e.g., minimum subcomponent mass or overall total structural mass) are customizable depending on the user's needs. JacketSE also allows for parametric investigations and sensitivity analyses of both external factors and geometric variables that may drive the characteristics of the structure, thereby illustrating their impact on the mass, stiffness, blade/support clearance, strength, reliability, and expected costs.

When used for optimization, the tool can size ODs and t's for piles, legs, and braces; other design variables that may be optimized are batter angle, pile embedment, tower base and top diameters, wall thickness schedule, and tapering height. The design parameters (fixed inputs to the tool) include: water depth, deck and hub height, design wind speed, design wave height and period, and soil characteristics (stratigraphy of undrained shear strength, friction angles, and specific weight). Loads from the rotor nacelle assembly (RNA) are input to the model either from other WISDEM modules or directly from the user. The user must also provide acceptable ranges for the design variables, such as, maximum tower OD; minimum and maximum *DTR*s for the various members; and maximum allowed footprint at the seabed. Additional design criteria and constraints can be employed by the user if desirable.

As part of a system study within WISDEM, JacketSE allows for the full gamut of component investigations to arrive at optimum LCOE wind turbine and/or power plant layout. For example, JacketSE can produce a design that meets blade-tower/substructure clearance criteria while also meeting mass or cost targets.

The model has undergone preliminary verification (Damiani and Song 2013; Damiani et al. 2016), but an extensive campaign against other codes and industry data has yet to be performed. A future version of the model will include refined fatigue treatment, hydrodynamics loading, and automatic selection of standard dimensions for the various subcomponents.

This document discusses the model details in Section 2, with an overview of the verification and validation efforts in Section 3. A simple case study showing the key capabilities of the software is presented in Section 4. A summary of the development thus far and recommended future research activities are provided in Section 5.

[1] Patented jacket configuration by OWEC Tower AS.

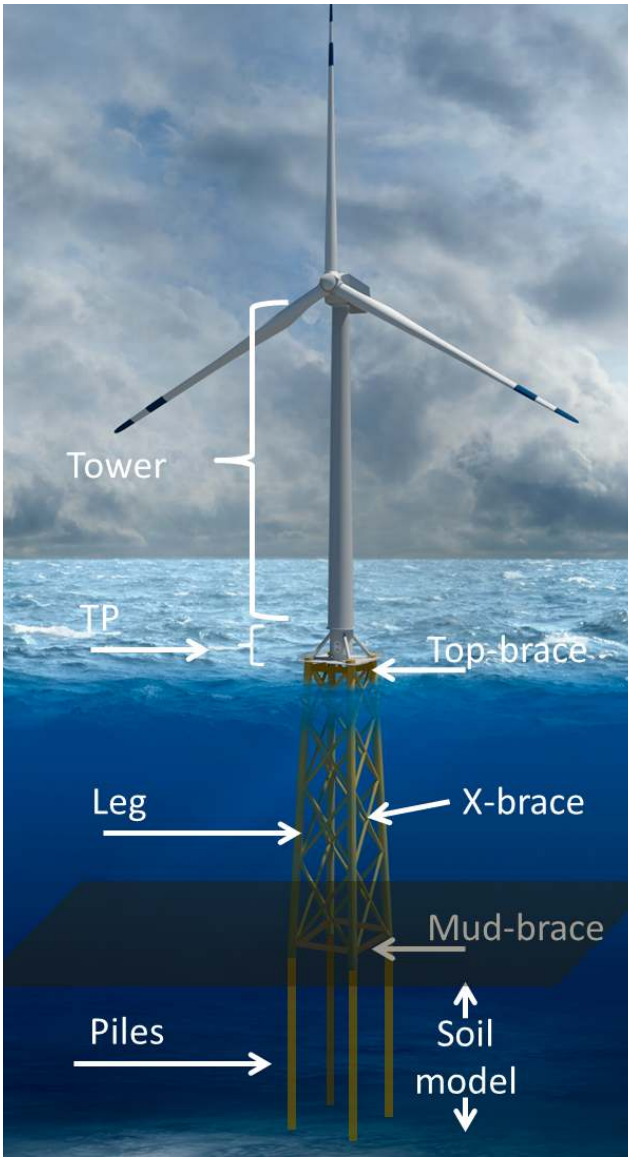

Figure 1. Diagram showing the main geometric and structural components JacketSE refers to. ***Original illustration by Joshua Bauer, NREL (modified here)***

2 Lattice Model Description

JacketSE is based on a modular code framework and primarily consists of the following submodules: geometry-definition; load calculation; soil-pile-interaction model; FEA model; structural code check; and optimization. A number of simplifications have been incorporated to allow for rapid analyses of multiple configurations on a personal computer. As such, complex hydrodynamics and associated variables (e.g., tidal range, marine growth, and member-to-member hydrodynamic interaction) are ignored, and fatigue assessments are not carried out. Although these aspects can very well drive the design of certain subcomponents and of the overall structure (Cordle, McCann, and de Vries 2011; Zwick et al. 2014; Molde, Zwick, and Muskulus 2014), it is believed that the main structural and mass characteristics should still be captured by the simplified model for the sake of preliminary design assessments and trade-off studies, and with a level of accuracy limited to those goals. Further details on the code can be found at https://github.com/WISDEM/JacketSE.git and Damiani and Song (2013). Additional conservatism can be provided by the choice of drag (c_d) and added mass (c_m) coefficients, the choice of a worst-case loading scenario, and additional safety factors. For example: for the substructure, the c_d and c_m values could be doubled with respect to those recommended by API (2014); the tower drag c_d could be set equal to 2 to account for TP drag; and the wave loads calculated on the main legs could be multiplied by a factor of four to account for hydrodynamics effects on secondary members of the substructure otherwise not considered. Preliminary comparisons of loads to the peak loads from dynamic simulations performed with SACS (a commercial package by Bentley for the analysis of offshore fixed-bottom structures) and FAST v8 (NREL's aero-elastic tool) of similar substructure configurations led to the choice of those coefficients. Future studies will employ a refined FLS treatment.

The coupled geometry modules are implemented as components within OpenMDAO[1] and they include (see also Figure 1):

- Piles
- Legs
- Mud-braces
- X-braces
- Top-braces
- TP
- Tower.

A series of inputs are needed to define the entire geometry. Some of those inputs are parameters (i.e., they won't change throughout an optimization process), whereas others can be defined as design variables to be optimized. For example, the height of the deck above mean sea level (MSL), water depth, wave height, and nominal gust speed are fixed parameters; batter, deck width, tower-waist height, and leg OD are key geometric variables. In Table 1, examples of the key geometric inputs are given, and more are provided in the subsequent Sections.

2.1 Member Definition and Tube Class

Most members within the substructure and tower can be represented as tubular beam elements. As such, a *tube* object class is defined. The tube object is fully defined by (see also Table 2): ODs, t's, k_{buck}'s (buckling parameter or effective length factor), l_{tube}'s (tube object unsupported length), and material properties. The latter are defined via a dedicated object class (*mat*), which contains E (Young's modulus), G (shear modulus), ρ (material density), f_y (characteristic yield strength), and calculates the associated ν (Poisson's ratio). Related to this class are cross-sectional properties such as surface area, shear area, area moments of inertia, bending moduli, cross-section radius of

[1] National Aeronautics and Space Administration software for multidisciplinary analysis and optimization

Table 1. Examples of JacketSE's Geometry Inputs

Input[(a)]	Type	Description	Default Value	Units
d_w	parameter	water depth	–	m
z_{dbot}	parameter	height of TP deck	16	m
z_{hub}	parameter	hub height	-	m
n_{legs}	parameter	number of legs in the substructure (equal to the number of piles)	4	–
n_{bays}	parameter	number of bays	5	–
CP_{fg}	parameter	flag indicating whether (True) or not (False) the legs are considered clamped at the seabed	False	–
VP_{fg}	parameter	flag indicating whether the piles are vertical (True) or battered (False)	True	–
PP_{fg}	parameter	flag indicating whether (True) or not (False) the piles are considered 'plugged'	False	–
TP_{lvl}	parameter	level of automatic build for the TP	5	–
wdr	parameter	allowance for weldments as a function of member diameter	0.5	m
$\mathbf{TP_{mas}}$	parameter	TP lumped mass, including mass, mass tensor (I_{xx}–I_{zz}) and CM offset from the center of the deck	–	kg, kg m^2
m_{RNA} and I_{xx}–I_{zz}	parameter	m_{RNA} and mass tensor	–	kg, kg m^2
$\mathbf{CM_{off}}$	parameter	distance vector from the tower-top flange to the CM of the RNA	–	m
ψ	parameter	rotor yaw angle about global z	45	deg
b	variable	two-dimensional batter, i.e., the vertical-to-horizontal ratio of the jacket-leg slope on a 2D projection	7	–
dck_w	variable	deck-side length	12	m
D_p	variable	pile outer diameter	1.5	m
t_p	variable	pile wall thickness	0.035	m
L_p	variable	pile embedment length	40	m
D_{leg}	variable	leg outer diameter	1.5	m
t_{leg}	variable	leg wall thickness	0.0254	m
D_{mbrc}	variable	mud-brace outer diameter	1	m
t_{mbrc}	variable	mud-brace wall thickness	0.0254	m
D_{xbrc}	variable	x-brace outer diameter	0.8	m
t_{xbrc}	variable	x-brace wall thickness	0.0254	m
D_{gir}	variable	TP girder OD	1	m
t_{gir}	variable	TP girder t	0.0254	m
D_b	variable	tower-base OD	5	m
D_t	variable	tower-top OD	3	m

[a] Symbols used in this manual might differ from those used in the actual code, which are typeset from alphanumeric, standard-set characters, but they can be easily referred to the variable names in the current version of JacketSE. See https://github.com/WISDEM/JacketSE.git.

Table 2. Tube Class Variables and Parameters Used in the Definition of the Members in JacketSE

Input[a]	Type	Description	Units
OD	variable	outer diameter	m
t	variable	wall thickness	m
l_{tube}	parameter	tube object unsupported length	m
n_{div}	parameter	number of elements in the member under consideration	–
k_{buck}	parameter	buckling parameter or effective length factor	–
ρ	parameter	material density	$\mathrm{kg\,m^{-3}}$
E	parameter	Young's modulus	$\mathrm{N\,m^{-2}}$
G	parameter	shear modulus	$\mathrm{N\,m^{-2}}$
ν	parameter	Poisson's ratio	m
f_y	parameter	characteristic yield strength	$\mathrm{N\,m^{-2}}$

[a] Symbols used in this manual might differ from those used in the actual code, which are typeset from alphanumeric, standard-set characters, but they can be easily referred to the variable names in the current version of JacketSE. See https://github.com/WISDEM/JacketSE.git.

gyration (r_{gyr}), and slenderness ratio (KLR) that are used by the FEA solver. The slenderness ratio (used in buckling verifications) is defined as:

$$KLR = \frac{k_{buck} l_{tube}}{r_{gyr}} \tag{2.1}$$

A member is defined as a joint-to-joint structural entity (e.g., the member between two adjacent k-joint along the leg). Each member can be given different material properties (e.g., to use different steels for the legs and x-braces in the first jacket bay).

Multiple elements along each member may be defined to reduce discontinuities in the FEA mesh element sizes going from one member to another. For the tower component, multiple elements are used to approximate the taper in OD and t. In future versions of the code, this approach will help account for tapered members in the substructure as well. The FEA solver can directly return the internal loads at various stations along a beam element, but this capability is not currently exploited. For this reason, adopting a number of elements greater than one may be used to evaluate the stress level in the substructure member with the current version of JacketSE.

2.2 Soil

The soil is described as either cohesive (clay) or cohesionless (sandy), and by a simple stratigraphy table (see Table 3), which includes soil level depth (z_d), unit weight (γ_s), undrained shear strength (c_u), friction angles (ϕ_s), and an average angle value representing steel-to-soil friction (δ_s). Soil characteristics affect the axial pile capacity and the stiffness of the soil-pile system described below.

In JacketSE, many assumptions are made to simplify the physics and behavior of the soil and foundation. In the future, these models will be upgraded with higher fidelity ones. One of the main assumptions concerns the variation of the E_s—soil modulus or modulus of subgrade reaction ($\mathrm{N\,m^{-2}}$)—with depth below the seabed. An E_s's linear trend, which is largely adopted in JacketSE, is mostly representative of consolidated clays, whereas cohesionless soils tend to have a parabolic trend. Corrections are employed when sandy soils are considered, as in the Pender's method to calculate the pile-head stiffness (described in Section 2.3.2), and in the calculation of the coefficient of subgrade reaction in Matlock and Reese's method (see Section 2.3.2). It is further assumed, following Murthy

Table 3. Typical Stratigraphy Arrangement used by JacketSE

Depth m	γ_s N m^{-3}	c_u N m^{-2}	ϕ_s deg	δ_s deg
-3	10,000	60,000	36	25
-5	10,000	60,000	33	
-7	10,000	60,000	26	
-15	10,000	60,000	37	
-30	10,000	60,000	35	
-50	10,000	60,000	37.5	

(2002), that the E_s can be described in terms of k_s (coefficient of subgrade reaction):

$$E_s = k_s z_d \tag{2.2}$$

A default partial safety factor (PSF) equal to two is set for calculations involving soil properties, but, given the uncertainty in the geotechnical data and modeling assumptions, larger values are encouraged.

2.3 Piles

The piles can be either vertical or driven through the legs, and therefore slanted (battered), as is normal practice in the oil and gas (O&G) industry. In the case of a more common offshore wind jacket, the piles are either driven through a template on the ground prior to lowering and grouting the lattice (prepiled jacket version), or driven through and grouted to pile sleeves that are built in at the foot of each leg (postpiled version). JacketSE assumes that the members' input accounts for any eventual concentric, grouted configuration. Thus, if the piles are driven through the legs, the input must provide equivalent material properties and wall thickness for the legs' members to best model the stiffness of the nonhomogeneous pile-grout-leg cross section. In the case of vertical piles, the physical connection (see Figure 2) is replaced by an idealized moment connection node between the pile and the leg, but user's input should at least account for the extra mass associated with the grouted connection. Similarly, in the case of a connection via the sleeve plate, JacketSE does not automatically include these subcomponents, and the user should make provisions for extra steel at the base of the jacket. Future releases will improve these aspects of the substructure and foundation modeling.

The piles are fully identified by b (the two-dimensional batter, i.e., the vertical-to-horizontal ratio of the jacket-leg slope on a $2D$ projection), D_p (the pile outer diameter), t_p (the pile wall thickness), L_p (the pile embedment length), and PP_{fg}, which is a boolean flag that indicates whether or not they are considered 'plugged' (see also Tables 1, 2, and 4). To determine the embedded length of the pile, JacketSE performs an axial load capacity check, which normally drives the design of jacket piles. Piles should also be verified for lateral capacity, and in the future this verification will be included. The piles properties are also used, together with the soil properties, to estimate equivalent spring constants at the leg bottom.

In general, the stability of the piles at the seabed should also be verified, in which head displacement and rotation would be checked against allowable values from the standards. This is not done in this version of the code, and will be included in a future version along with lateral stability and capacity checks.

2.3.1 Axial Capacity

The normal force exchanged at the head of the pile must be reacted by friction along the outer surface of the pile (also called shaft friction) and by the contact force at the pile tip. In the case of unplugged piles, friction developed

Table 4. Variables and Parameters Used in the Definition of the Pile Members in JacketSE

Input[a]	Type	Description	Default Value	Units
D_p	variable	pile outer diameter	1.5	m
t_p	variable	pile wall thickness	0.035	m
CP_{fg}	parameter	flag indicating whether (True) or not (False) the legs are considered clamped at the seabed	False	–
VP_{fg}	parameter	flag indicating whether the piles are vertical (True) or battered (False)	True	–
PP_{fg}	parameter	flag indicating whether (True) or not (False) the piles are considered 'plugged'	False	–
z_{lb}	parameter	elevation of the leg-toe above the seabed	0	m
$n_{div,pile}$	parameter	number of elements in the pile member	0	–
k_{buck}	parameter	buckling parameter or effective length factor	1	–
ρ	parameter	material density	7805	$\mathrm{kg\,m^{-3}}$
E	parameter	Young's modulus	2.1e11	$\mathrm{N\,m^{-2}}$
G	parameter	shear modulus	7.895e10	$\mathrm{N\,m^{-2}}$
ν	parameter	Poisson's ratio	0.3	–
f_y	parameter	characteristic yield strength	345	$\mathrm{N\,m^{-2}}$

[a] Symbols used in this manual might differ from those used in the actual code, which are typeset from alphanumeric, standard-set characters, but they can be easily referred to the variable names in the current version of JacketSE. See https://github.com/WISDEM/JacketSE.git.

Table 5. Design Parameters for Cohesionless Soil (API 2014)

Soil Density	δ_s deg	f_{max} kPa	N_q	$q_{p,max}$ MPa
Very loose-medium	15	47.8	8	1.9
Loose-dense	20	67	12	2.9
Medium-dense	25	81.3	20	4.8
Dense-very dense	30	95.7	40	9.6
Dense-very dense	35	114.8	50	12

along the inner surface may also be included in the axial capacity of the pile. The ultimate bearing capacity, Q_d, is calculated following API (2014) as:

$$Q_d = Q_f + Q_p = fA_s + q_p A_p \tag{2.3}$$

where Q_f is the skin friction resistance, Q_p is the end bearing resistance, f is the skin friction, A_s is the side surface area of the pile, q_p is the unit end bearing capacity, and A_p is the surface area of the pile tip.

Depending on whether the soil is considered cohesive or cohesionless, two different methods are employed to calculate the shaft friction.

For cohesive soils, the procedure makes use of the ψ_s and α_s factors defined as:

$$\begin{cases} \alpha_s = \min\left(1, 0.5\psi_s^{-0.5}\right) & \text{if} \quad \psi_s \leq 1 \\ \alpha_s = \min\left(1, 0.5\psi_s^{-0.25}\right) & \text{if} \quad \psi_s > 1 \end{cases} \quad \text{with} \quad \psi_s = c_u / p'_o \tag{2.4}$$

where p'_o is the overburden pressure at the depth of interest.

For cohesionless soils, f is calculated as:

$$f = K_{API} p'_o \tan\delta_s \tag{2.5}$$

where K_{API} is the coefficient of lateral earth pressure, which can be taken as 1.0 for plugged and 0.8 for unplugged piles.

The end bearing capacity is also calculated differently for the two soil types. For clay soils, the unit end bearing is given by:

$$q_p = 9c_u \tag{2.6}$$

For sandy soils, q_p is given by Eq. (2.7) and in any case limited by $q_{p,max}$ given in Table 5:

$$q_p = p'_o N_q \tag{2.7}$$

where N_q is a dimensionless bearing capacity factor and recommended values are given in Table 5. The total end bearing capacity is calculated based on the pile wall annulus, or the gross cross-sectional area if the pile is considered plugged.

2.3.2 Pile Head Stiffness

To account for the soil-pile interaction in a linearized fashion, two models are available in JacketSE: 1) Matlock and Reese (1960) and 2) Pender (1993). Through these methods, an equivalent stiffness matrix (or the inverse of a

Table 6. Coefficient of Subgrade Reaction, k_s, for Cohesionless Soils as a Function of Friction Angle (from API 2014)

ϕ_s (deg)	28	29	30	33	36	38	40	42.5	45
k_s (below water table, MN m^{-3})	1.36	3.39	9.33	16.54	25.45	33.08	42.41	49.2	60.23
k_s (above water table, MN m^{-3})	0.1	3.39	12.72	25.02	43.26	57.68	75.92	88.22	102.64

flexibility matrix) is devised to be applied at the leg foot:

$$\begin{bmatrix} F_{p,x} \\ F_{p,y} \\ F_{p,z} \\ M_{p,x} \\ M_{p,y} \\ M_{p,z} \end{bmatrix} = \begin{bmatrix} k_{xx} & 0 & 0 & 0 & k_{x\theta_y} & 0 \\ 0 & k_{yy} & 0 & k_{y\theta_x} & 0 & 0 \\ 0 & 0 & k_{zz} & 0 & 0 & 0 \\ 0 & k_{\theta_x y} & 0 & k_{\theta_x\theta_x} & 0 & 0 \\ k_{\theta_y x} & 0 & 0 & 0 & k_{\theta_y\theta_y} & 0 \\ 0 & 0 & 0 & 0 & 0 & k_{\theta_z\theta_z} \end{bmatrix} \begin{bmatrix} u_{p,x} \\ u_{p,y} \\ u_{p,z} \\ \theta_{p,x} \\ \theta_{p,y} \\ \theta_{p,z} \end{bmatrix} \tag{2.8}$$

where $F_{p,x}$-$F_{p,z}$ are the pile head forces, $M_{p,y}$-$M_{p,z}$ are the pile head moments, $u_{p,x}$-$u_{p,z}$ are the pile head displacements, $\theta_{p,x}$-$\theta_{p,z}$ are the pile head rotations, k_{xx} (=k_{yy} for symmetry)-k_{zz} are the forces at the pile head when unit displacements are imposed at the pile head, $k_{x\theta_y}$ (=$k_{y\theta_x}$ for symmetry) are the forces when unit rotations are imposed at the pile head, $k_{\theta_x y}$ (=$k_{\theta_y x}$ for symmetry) are the moments when unit displacements are imposed at the pile head, and $k_{\theta_x\theta_x}$ (=$k_{\theta_y\theta_y}$ for symmetry)-$k_{\theta_z\theta_z}$ are the moments when unit rotations are imposed at the pile head. For reciprocity, $k_{\theta_x y}$=$k_{y\theta_x}$, thus only five terms (k_{xx},k_{zz},$k_{x\theta_y}$,$k_{\theta_y\theta_y}$,$k_{\theta_z\theta_z}$) are unique in the stiffness matrix of Eq. (2.8).

The leg-to-pile connection is assumed to be of the grouted type, as shown in Figure 2, and not capable of securing head fixity. This assumption renders the connection and the soil-pile stiffness conservatively less rigid. The two semiempirical models are useful for design purposes, but a refined analysis is needed in detailed design, for which $p-y$ (nonlinear spring treatment of soil-pile lateral stiffness), $t-z$ (nonlinear spring treatment of soil-pile axial stiffness), and $Q-z$ (nonlinear spring treatment of soil-pile end-bearing, axial stiffness) curves should be considered (API 2014).

Based on a nondimensional analysis, Matlock and Reese (1960) identify a relative stiffness factor T_{mr}, as shown in Eq. (2.9), which in turn is used to obtain the flexibility matrix coefficients, as shown in Eq. (2.10):

$$\begin{aligned} T_{mr} &= \left[\frac{E_p J_{xx,p}}{k_s}\right]^{1/5} \\ \text{with} \quad E_s &= k_s z_d \end{aligned} \tag{2.9}$$

$$\begin{aligned} f_{xx} &= 2.43\frac{T_{mr}^3}{E_p J_{xx,p}} \\ f_{x\theta} &= f_{\theta x} = 1.62\frac{T_{mr}^2}{E_p J_{xx,p}} \\ f_{\theta\theta} &= 1.75\frac{T_{mr}}{E_p J_{xx,p}} \end{aligned} \tag{2.10}$$

where E_p is the pile Young's modulus, $J_{xx,p}$ is the pile cross-sectional, second area moment of inertia, and z_d is the depth below the seabed. Note that Eq. (2.9) assumes a linear dependence of E_s with z_d.

For sands, k_s may be determined by following the trend recommended by API (2014) as a function of relative density and friction angle, as shown in Table 6.

For cohesive soils, Bowles (1997) proposes values that are interpolated as a function of soil allowable bearing-capacity (q_a):

$$k_s = \begin{cases} 12000 + \frac{12000}{100\,\text{kPa}}(q_a - 100\,\text{kPa}) & \text{if} \quad q_a \le 200\,\text{kPa} \\ 24000 + \frac{24000}{600}(q_a - 200\,\text{kPa}) & \text{if} \quad 200\,\text{kPa} < q_a \le 800\,\text{kPa} \\ 48000 & \text{if} \quad q_a > 800\,\text{kPa} \end{cases} \tag{2.11}$$

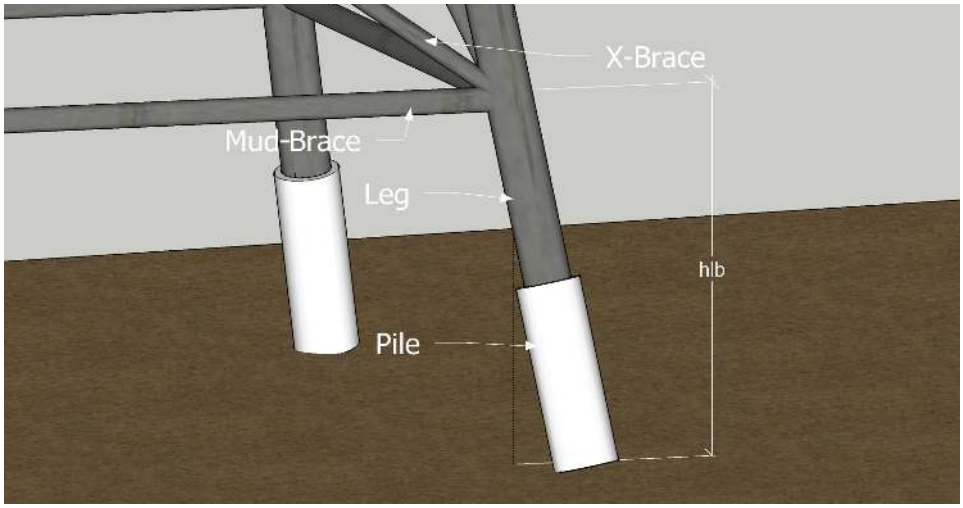

(a)

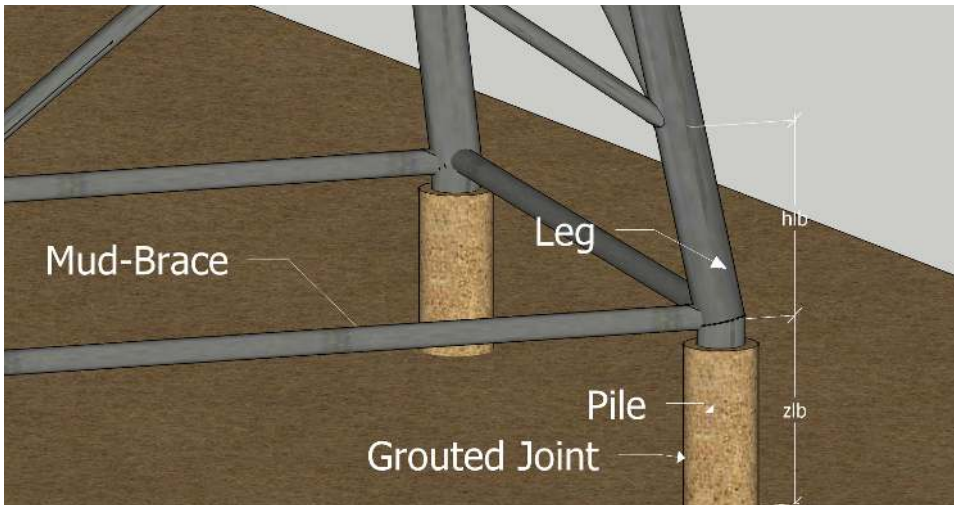

(b)

Figure 2. Diagrams of the grouted connections at the leg footing shown together with the definitions of z_{lb} and h_{lb}, see text for more details: (a) shows the slanted (battered) pile configuration; (b) is the vertical pile configuration.

where units for k_s are $\mathrm{kN\,m^{-3}}$.

In Pender's method, a modulus ratio, K_p, and an active length, L_a, of the pile are first defined as:

$$K_p = \frac{E_p}{E_s(D_p)} = \frac{E_p}{k_s D_p} \tag{2.12}$$

$$L_a = 1.3 D_p K_p^{0.222} \tag{2.13}$$

If the pile can be considered 'long' (i.e., flexible), then the flexibility coefficients become:

$$\begin{cases} \text{if} \quad L_p \geq L_a: \\ \quad \begin{cases} f_{xx} = 2.14 \dfrac{K_p^{-0.29}}{E_s(D_p) D_p} \\ f_{x\theta} = f_{\theta x} = 3.43 \dfrac{K_p^{-0.53}}{E_s(D_p) D_p^2} \quad \text{for cohesionless soils (quadratic variation of } E_s \text{ with } z_d) \\ f_{\theta\theta} = 12.16 \dfrac{K_p^{-0.77}}{E_s(D_p) D_p^3} \end{cases} \\ \text{or} \\ \quad \begin{cases} f_{xx} = 3.2 \dfrac{K_p^{-0.333}}{E_s(D_p) D_p} \\ f_{x\theta} = f_{\theta x} = 5 \dfrac{K_p^{-0.556}}{E_s(D_p) D_p^2} \quad \text{for cohesive soils (linear variation of } E_s \text{ with } z_d) \\ f_{\theta\theta} = 13.6 \dfrac{K_p^{-0.778}}{E_s(D_p) D_p^3} \end{cases} \end{cases} \tag{2.14}$$

If the pile can be considered 'short' (i.e., rigid), then:

$$\begin{cases} \text{if} \quad L_p \leq 0.07 D_p \sqrt{K_p}: \\ f_{xx} = 0.7 \dfrac{\mathscr{L}^{-0.333}}{E_s(D_p) D_p} \\ f_{x\theta} = f_{\theta x} = 0.4 \dfrac{\mathscr{L}^{-0.88}}{E_s(D_p) D_p^2} \\ f_{\theta\theta} = 0.6 \dfrac{\mathscr{L}^{-1.67}}{E_s(D_p) D_p^3} \end{cases} \tag{2.15}$$

where $\mathscr{L}$ is the ratio of the pile length to its diameter.

For intermediate piles—i.e., those with lengths between the bounds shown in Eqs. (2.14) and (2.15)—, the flexibility coefficients are approximated by applying a 1.25 factor to those of Eq. (2.14).

Note that both of these treatments assume a linear dependence of E_s with z_d.

To get the terms k_{xx}, $k_{x\theta_y}$, and $k_{\theta_y\theta_y}$ of the pile head stiffness matrix to apply at the seafloor, the flexibility matrix is inverted to give:

$$\begin{bmatrix} k_{xx} & k_{x\theta_y} \\ k_{\theta_y x} & k_{\theta_y\theta_y} \end{bmatrix} = \frac{1}{f_{xx} f_{\theta\theta} - f_{x\theta}^2} \begin{bmatrix} f_{\theta\theta} & -f_{x\theta} \\ -f_{\theta x} & f_{xx} \end{bmatrix} \tag{2.16}$$

An additional, axial spring constant is computed following Pender (1993) for the linear variation of E_s with depth, and given by:

$$k_{zz} = 1.8 k_s L_p D_p^{0.55} \mathscr{R}^{-\frac{\mathscr{L}}{\mathscr{R}}} \tag{2.17}$$

$$\mathscr{R} = \frac{E_p}{k_s L_p} \tag{2.18}$$

Finally, the torsional stiffness is approximated following Randolph (1981) as:

$$k_{\theta_z\theta_z} \simeq \frac{\pi\sqrt{2}G_{s,c}D_p^3}{16}\left(\frac{\hat{G}_p}{G_{s,c}}\right)^{0.5} \tag{2.19}$$

where L_c is the pile critical embedment length for torsion response, $G_{s,c}$ is the soil shear modulus at torsional critical depth, and $\hat{G}_p$ is the equivalent shear modulus used for piles. These quantities are calculated as follows:

$$\hat{G}_p = \frac{32G_pJ_{xx,p}}{\pi D_p^4} \tag{2.20}$$

$$G_{s,c} = G_s(L_c) \tag{2.21}$$

$$L_c \simeq \frac{D_p}{16}\left(\frac{2(1+\nu_s)\hat{G}_p}{k_sD_p}\right)^{1/3} \tag{2.22}$$

where ν_s is the soil Poisson's ratio.

If the piles are battered, the legs should be defined accounting for the presence of the pile, i.e., they should satisfy inequality (2.23) (Chakrabarti 2005):

$$D_{leg} - 2t_{leg} \geq D_p + 0.09\,\text{m} \tag{2.23}$$

where D_{leg} and t_{leg} denote the jacket leg's OD and t, respectively. Furthermore, to account for the batter, the stiffness matrix is rotated by ψ_{rot} about the global z, and by ϕ_{rot} about the resulting new x axis, to arrive at:

$$K_g = C_{l2g} \quad K_l \quad C_{l2g}{}^T \tag{2.24}$$

where C_{l2g} is given by:

$$C_{l2g} = \begin{bmatrix} \cos\gamma_{in}\cos\alpha_{bat,3D} & -\sin\gamma_{in} & -\sin\alpha_{bat,3D}\cos\gamma_{in} \\ \sin\gamma_{in}\cos\alpha_{bat,3D} & \cos\gamma_{in} & -\sin\alpha_{bat,3D}\sin\gamma_{in} \\ \sin\alpha_{bat,3D} & 0 & \cos\alpha_{bat,3D} \end{bmatrix} \tag{2.25}$$

where γ_{in} is the angle described by the horizontal projection of one side of the jacket base and a line connecting the center of the polygon at the base and one end of that side ($= \pi/2$ for four-legged jackets), and $\alpha_{bat,3D}$ is the three-dimensional batter angle (see Figure 3):

$$\alpha_{bat,3D} = \arctan\frac{\sqrt{2}}{b} \tag{2.26}$$

2.4 Legs

Each leg is made up of n_{bays}+2 members (n_{bays} is the number of bays), which can be individually defined in terms of OD, t, k_{buck} (default=1), and material properties (see also Table 7). Normally, one set of dimensions is used for multiple bays to reduce fabrication complexity, but the code allows for tapered legs.

As mentioned earlier, the presence of internal piles, in the case of battered ones, requires the user to provide adequate equivalent material properties and wall thickness for the leg members. For instance, a simple approach calls for an equivalent member that has the same mass, axial, and bending stiffness as the original concentric member arrangement.

The geometry of the legs is completely tied to the overall jacket layout. With a few given values for the overall geometric variables (e.g., deck-side length, height of the jacket available to the bays, and two-dimensional batter),

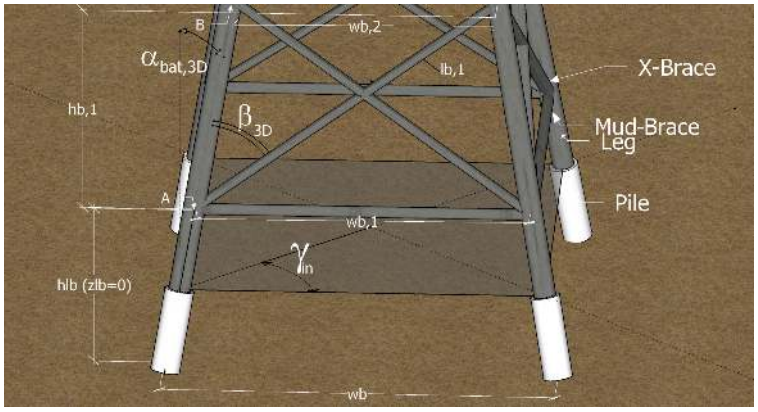

Figure 3. Defintions of key variables in the geometry used by JacketSE

Table 7. Variables and Parameters Used in the Definition of the Leg Members in JacketSE

Input[a]	Type	Description	Default Value	Units
D_{leg}	variable	leg outer diameter	1.5	m
t_{leg}	variable	leg wall thickness	0.0254	m
z_{lb}	parameter	elevation of the leg-toe above the seabed	0	m
h_{lb}	parameter	distance from the leg-toe to the first joint with an x-brace	$1.5 \cdot D_{leg}$	m
$n_{div,leg}$	parameter	number of elements in the leg member	3	–
k_{buck}	parameter	buckling parameter or effective length factor	1	–
ρ	parameter	material density	7805	$\mathrm{kg\,m^{-3}}$
E	parameter	Young's modulus	2.1e11	$\mathrm{N\,m^{-2}}$
G	parameter	shear modulus	7.895e10	$\mathrm{N\,m^{-2}}$
ν	parameter	Poisson's ratio	0.3	–
f_y	parameter	characteristic yield strength	345	$\mathrm{N\,m^{-2}}$

[a] Symbols used in this manual might differ from those used in the actual code, which are typeset from alphanumeric, standard-set characters, but they can be easily referred to the variable names in the current version of JacketSE. See https://github.com/WISDEM/JacketSE.git.

the joints and nodes of the legs can be identified via trigonometric functions—see also Eq. (2.32). The joints are the intersections of leg members with either braces or other members. The nodes are defined as end nodes of the FEA elements.

First, the bay heights must be calculated. The width of the jacket base (length of one side) at the seabed and the horizontal distance between the leg-to-brace joints at bay 1 (bottom bay), i.e., bay-1 bottom width, are given by (see also Figure 3):

$$w_b = dck_w - 2D_{lt}/2(1+wdr) + 2(d_w + z_{dbot})/b \tag{2.27}$$

$$w_{b,1} = w_b - 2\tan\left[\alpha_{bat,2D}\right](z_{lb} + h_{lb}) \tag{2.28}$$

$$\tag{2.29}$$

where dck_w is the deck-side length, d_w is the water depth, D_{lt} is the leg top OD, wdr is the allowance for weldments as a function of member diameter, z_{dbot} is the deck underside elevation MSL, $\alpha_{bat,2D}$ is the two-dimensional batter angle—that corresponds to b—, z_{lb} is the elevation of the leg-toe above the seabed, and h_{lb} is the distance from the leg-toe to the first joint with an x-brace. The widths of each further bay can be recursively calculated as in Eq. (2.30):

$$w_{b,i} = w_{b,i-1}\left[1 - 2\tan(\alpha_{bat,2D})\frac{\tan(\pi/2 - \beta_{2D} - \alpha_{bat,2D})}{1 + \tan(\alpha_{bat,2D})\tan(\pi/2 - \beta_{2D} - \alpha_{bat,2D})}\right] \tag{2.30}$$

It can also be proved that the height of each bay ($h_{b,i}$) can be written as:

$$h_{b,i} = w_{b,i}\frac{\tan(\pi/2 - \beta_{2D} - \alpha_{bat,2D})}{1 + \tan(\alpha_{bat,2D})\tan(\pi/2 - \beta_{2D} - \alpha_{bat,2D})} \tag{2.31}$$

where β_{2D} is the brace-to-leg angle as measured on a vertical projection, which is an unknown, but is considered fixed throughout the bays for ease of manufacturability. By making use of the above definitions and simultaneously solving the system of equations in Eq. (2.32), the β_{2D} angles can be calculated:

$$\begin{cases} h_{jckt} &= z_{dbot} + d_w - z_{lb} \\ \mathbf{h_{bys}} &= h_{jckt} - h_{lb} \\ \mathbf{h_{bys}} &= \sum_1^{n_{bays}} h_{b,i} \end{cases} \tag{2.32}$$

In Eq. (2.32), h_{jckt} is the height of the jacket available to the bays, and $\mathbf{h_{bys}}$ is the array containing the bay heights.

The actual brace-to-leg angle β_{3D} can be calculated from the extended Pythagorean theorem:

$$\begin{cases} w_{b,2}^2 - \left(AB^2 + l_{b,1}^2 - 2 * AB * l_{b,1}\cos(\beta_{3D})\right) = 0 \quad \text{with} \\ AB = \frac{h_{b,1}}{\cos(\alpha_{bat,3D})} \\ l_{b,1} = \sqrt{h_{b,1}^2 + \left(w_{b,1} - h_{b,1}\tan(\alpha_{bat,2D})\right)^2 + \left(h_{b,1} * \tan(\alpha_{bat,2D}) * \tan(\gamma_{in})\right)^2} \\ w_{b,2} = w_{b,1} - 2h_{b,1}\tan(\alpha_{bat,2D}) \\ h_{b,1} = w_{b,1}\frac{\tan(\pi/2 - \beta_{2D} - \alpha_{bat,2D})}{1 + \tan(\alpha_{bat,2D}) * \tan(\pi/2 - \beta_{2D} - \alpha_{bat,2D})} \end{cases} \tag{2.33}$$

Note that Eq. (2.33) is numerically solved for β_{3D}, and AB is the distance between the first two leg joints at the bottom bay, $w_{b,2}$ is the second bay width, $l_{b,1}$ is the length of the bottom x-brace, and $h_{b,1}$ is the height of the bottom bay.

Once $\mathbf{h_{bys}}$ has been determined, the joints' coordinates and the internal nodes for the legs and the braces can be calculated. For the first leg, the joint coordinates are given by:

$$\begin{cases} x_{leg_i} = -w_b/2 + \frac{z_{leg} - z_{lb}}{b} \\ y_{leg_i} = x_{leg_i}\tan\gamma_{in} \\ z_{leg_i} = z_{lb} + \sum_1^i h_{b,i} \\ \text{with} \quad i = 1..n_{bays} \end{cases} \tag{2.34}$$

Table 8. Variables and Parameters Used in the Definition of the X-brace Members in JacketSE

Input[(a)]	Type	Description	Default Value	Units
D_{xbrc}	variable	x-brace outer diameter	0.8	m
t_{xbrc}	variable	x-brace wall thickness	0.0254	m
$n_{div,xbrc}$	parameter	number of elements in the x-brace member	1	–
k_{buck}	parameter	buckling parameter or effective length factor	0.8	–
ρ	parameter	material density	7805	$\mathrm{kg\,m^{-3}}$
E	parameter	Young's modulus	2.1e11	$\mathrm{N\,m^{-2}}$
G	parameter	shear modulus	7.895e10	$\mathrm{N\,m^{-2}}$
ν	parameter	Poisson's ratio	0.3	–
f_y	parameter	characteristic yield strength	345	$\mathrm{N\,m^{-2}}$

[a] Symbols used in this manual might differ from those used in the actual code, which are typeset from alphanumeric, standard-set characters, but they can be easily referred to the variable names in the current version of JacketSE. See https://github.com/WISDEM/JacketSE.git.

The other legs' coordinates are calculated starting from the above ones and rotating them about global z by the γ_{in} angle and repeating the operation for $n_{legs}-1$ times, where n_{legs} is the number of legs in the substructure (equal to the number of piles). Internal nodes are calculated by subdividing the obtained joints' coordinates proportionally to the user-supplied number of elements ($n_{div,leg}$). The material properties are also replicated for all the elements, so that *tube* objects can be produced for each of them.

2.5 X-Braces

With the leg joints defined, the x-braces are determined starting from the joints of two adjacent legs, and are assigned their respective inputs, namely ODs, t's, k_{buck} (default=0.8), and material properties (see also Table 8).

X-joints are defined at the three-dimensional intersections between the brace pairs, and calculated as in Eq. (2.35) (see also Figure 4):

$$\begin{cases} \underline{AB}_c = \overline{A_1A_2} \times \overline{B_1B_2} \\ \underline{A}_0 = \underline{A}_1 + \dfrac{n_A}{\underline{AB}_c}\overline{A_1A_2} \\ \text{with} \quad n_A = \overline{B_1B_2} \times \overline{B_1A_1} \cdot \underline{AB}_c \end{cases} \tag{2.35}$$

where A_1 and A_2 are the two joints at the ends of one of the two braces in the pair, B_1 and B_2 are the analog joints for the other brace, $\underline{AB}_c$ is the vector resulting from the cross product of $\overline{A_1A_2}$ and $\overline{B_1B_2}$, n_A is an auxiliary quantity, and $\underline{A}_0$ is the set of new coordinates for the x-joint.

Just like for the legs, if the input requests multiple elements ($n_{div,xbrc} > 1$), then new nodes are created by proportionally subdividing the coordinates of the joints in the member defined between the brace-leg joint and the x-joint.

The braces must satisfy a few constraints that are derived from engineering experience (Chakrabarti 1987) and

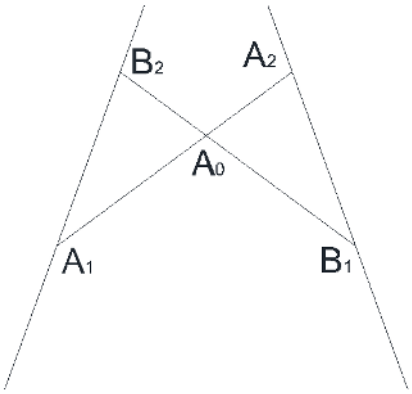

Figure 4. Schematics of the intersection between two x-braces

shown in Eq. (2.36):

$$\begin{cases} A_{brc} \geq 0.1 A_{leg} \\ D_{xbrc} \geq 0.3 D_{leg} \\ \frac{D_{xbrc}}{t_{xbrc}} \geq 31 \\ \frac{D_{xbrc}}{t_{xbrc}} \leq hydc = \frac{250.}{(3.28 d_w)^{0.33}} \\ KLR_{brc} \leq KLR_{max} = 70 - 80 \end{cases} \tag{2.36}$$

where A_{brc} the brace cross-sectional area, A_{leg} is the leg cross-sectional area, KLR_{brc} is the brace KLR, and $hydc$ is the hydrostatic constant. The first inequality of Eq. (2.36) ensures a rigid truss behavior of the bay and therefore an adequate shear transfer from leg to leg; the second constraint improves the capacity of the joints; the third constraint ensures the manufacturability of the brace and ensures positive buoyancy; the fourth inequality virtually removes hydrostatic problems; and the last constraint in Eq. (2.36) improves the axial capacity of the brace and renders the material utilization more efficient.

2.6 Mud-Brace

The mud-brace is a horizontal brace placed near the pile-to-leg joint. The mud-brace relieves the stress concentration at the pile head, and further increases the torsional stiffness of the substructure. The mud-brace is fully defined by its OD, t, k_{buck} (default=0.8), and material properties (see also Table 9). The position of the mud-brace changes depending on the pile configuration (see also Figure 2). If the piles are of the prepiled, vertical type, then the mud-brace joint with the leg is located at the assumed pile-to-leg joint. In the case of battered, in-leg piles, the mud-brace is joined to the leg at the bottom x-brace joints.

Like other members, the mud-brace may be subdivided into multiple elements via the input $n_{div,mud}$. The same constraints as in Eq. (2.36) apply to the mud-brace.

2.7 Top Brace

A set of horizontal braces at the top of the main lattice structure can be enabled as an option. The top braces connect the leg top joints together, and, similarly to the mud-braces, they relieve the stress concentration at the connection

Table 9. Variables and Parameters Used in the Definition of the Mud-brace Members in JacketSE

Input[a]	Type	Description	Default Value	Units
D_{mbrc}	variable	mud-brace outer diameter	1	m
t_{mbrc}	variable	mud-brace wall thickness	0.0254	m
$n_{div,mud}$	parameter	number of elements in the mud-brace member	1	–
k_{buck}	parameter	buckling parameter or effective length factor	0.8	–
ρ	parameter	material density	7805	$\mathrm{kg\,m^{-3}}$
E	parameter	Young's modulus	2.1e11	$\mathrm{N\,m^{-2}}$
G	parameter	shear modulus	7.895e10	$\mathrm{N\,m^{-2}}$
ν	parameter	Poisson's ratio	0.3	–
f_y	parameter	characteristic yield strength	345	$\mathrm{N\,m^{-2}}$

[a] Symbols used in this manual might differ from those used in the actual code, which are typeset from alphanumeric, standard-set characters, but they can be easily referred to the variable names in the current version of JacketSE. See https://github.com/WISDEM/JacketSE.git.

between the legs and TP stumps (defined in Section 2.8). The top bay's x-brace's OD and t are the default values for the top brace's OD and t, but the input can obviously be changed as needed. Completing the input set are k_{buck} (default value =0.8) and material properties (see also Table 9). Note, the top-brace may be omitted, with its role played by the TP girder.

Table 10. Variables and Parameters Used in the Definition of the Top-brace Members in JacketSE

Input[a]	Type	Description	Default Value	Units
D_{tbrc}	variable	top-brace outer diameter	D_{xbrc}	m
t_{tbrc}	variable	top-brace wall thickness	t_{xbrc}	m
$n_{div,tbrc}$	parameter	number of elements in the top-brace member	0 (not used)	–
k_{buck}	parameter	buckling parameter or effective length factor	0.8	–
ρ	parameter	material density	7805	$\mathrm{kg\,m^{-3}}$
E	parameter	Young's modulus	2.1e11	$\mathrm{N\,m^{-2}}$
G	parameter	shear modulus	7.895e10	$\mathrm{N\,m^{-2}}$
ν	parameter	Poisson's ratio	0.3	–
f_y	parameter	characteristic yield strength	345	$\mathrm{N\,m^{-2}}$

[a] Symbols used in this manual might differ from those used in the actual code, which are typeset from alphanumeric, standard-set characters, but they can be easily referred to the variable names in the current version of JacketSE. See https://github.com/WISDEM/JacketSE.git.

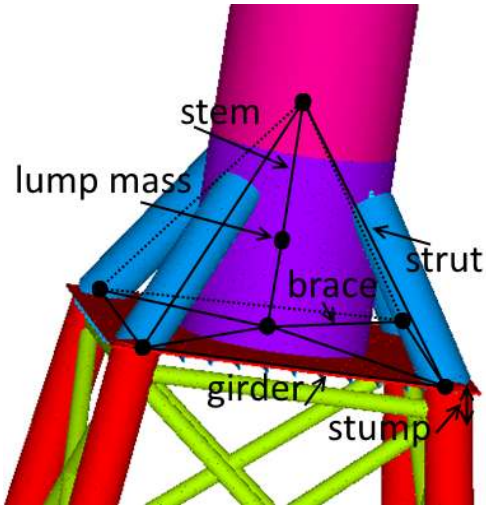

Figure 5. Diagram showing the structural simplification adopted by JacketSE to represent the TP with a frame of beams

2.8 TP

The TP structure is modeled by considering a frame of beams in lieu of the actual structure, as shown in Figure 5. A perimeter girder with two cross-braces make up the deck. A central beam (*stem*) represents the shell connecting to the base of the tower. Four additional beams (*struts*) support the shell from the corners.

The various subcomponents, or tubular beams, are described by material properties and ODs, t's, and k_{buck}'s (default value=0.8). The central stem needs also to be defined in terms of its length $\mathbf{h_{stem}}$, as its top node will connect to the tower. The stem can also accommodate a concentrated mass at the connection with the cross-braces. Additionally, vertical beams (*stumps*) can be used to represent spacers from the leg top-joints to the girders.

Key inputs for the TP are given in Table 11. Note that each subcomponent can be assigned different material properties, besides different values for the respective k_{buck}'s.

JacketSE provides a simpler way to assign the geometry of the TP submembers. There are five levels of automatic generation (TP_{lvl}) that can be selected:

1. $D_{strt} = D_{stmp} = D_{leg}$, $t_{strt} = t_{stmp} = t_{leg}$
2. as 1. plus $D_{gir} = D_{TPbrc} = D_{xbrc}$, $t_{gir} = t_{TPbrc} = t_{xbrc}$
3. $D_{gir} = D_{TPbrc} = D_{xbrc}$, $t_{gir} = t_{TPbrc} = t_{xbrc}$ only
4. $D_{gir} = D_{TPbrc}$, $t_{gir} = t_{TPbrc}$ only
5. as 1. + as 4.

For any of the above options, the elements of the arrays $\mathbf{D_{stem}}$ and $\mathbf{t_{stem}}$ are set to D_b and $f_{stem}t_b$, respectively, with f_{stem} given as input (=1.5 by default), and t_b being the tower-base t.

2.9 Tower

The tower is assumed to be made up of two main sections (see also Figure 6): a bottom segment with a constant cross section, and a top segment with both OD and t tapered. The main input variables are given in Table 12.

Table 11. Variables and Parameters Used in the Definition of the TP Members in JacketSE

Input[(a)]	Type	Description	Default Value	Units
D_{stmp}	variable	TP stump OD	D_{leg}	m
t_{stmp}	variable	TP stump t	t_{leg}	m
h_{stmp}	variable	TP stump length	0	m
D_{gir}	variable	TP girder OD	D_{xbrc}	m
t_{gir}	variable	TP girder t	t_{xbrc}	m
D_{TPbrc}	variable	TP cross-brace OD	D_{xbrc}	m
t_{TPbrc}	variable	TP cross-brace t	t_{xbrc}	m
D_{strt}	variable	TP strut OD	D_{leg}	m
t_{strt}	variable	TP strut t	t_{leg}	m
$\mathbf{D_{stem}}$	variable	array of TP central shell ODs (one per shell member)	D_b	m
$\mathbf{t_{stem}}$	variable	TP central shell t's (one per shell member)	$f_{stem}t_b$	m
$\mathbf{h_{stem}}$	variable	array of TP central shell lengths (one per shell member)	t_{leg}	m
TP_{lvl}	parameter	level of automatic build for the TP	5	–
$\mathbf{TP_{mas}}$	parameter	TP lumped mass, including mass, mass tensor (I_{xx}–I_{zz}) and CM offset from the center of the deck	-	kg, $\mathrm{kg\,m^2}$
n_{stem}	parameter	number of TP shell members	3	–
f_{stem}	parameter	ratio between the TP central-shell wall thickness and t_b	1.5	–
$n_{div,stmp}$	parameter	number of elements in each of the TP stumps	0 (not used)	–
$n_{div,strt}$	parameter	number of elements in each of the TP struts	1	–
$n_{div,gir}$	parameter	number of elements in each of the TP girder members	1	–
$n_{div,TPbrc}$	parameter	number of elements in each of the TP cross-brace members	1	–
k_{buck}	parameter	buckling parameter or effective length factor	0.8	–
$\rho^{(b)}$	parameter	material density	7805	$\mathrm{kg\,m^{-3}}$
$E^{(b)}$	parameter	Young's modulus	2.1e11	$\mathrm{N\,m^{-2}}$
$G^{(b)}$	parameter	shear modulus	7.895e10	$\mathrm{N\,m^{-2}}$
$\nu^{(b)}$	parameter	Poisson's ratio	0.3	–
$f_y{}^{(b)}$	parameter	characteristic yield strength	345	$\mathrm{N\,m^{-2}}$

[a] Symbols used in this manual might differ from those used in the actual code, which are typeset from alphanumeric, standard-set characters, but they can be easily referred to the variable names in the current version of JacketSE. See https://github.com/WISDEM/JacketSE.git.
[b] Material properties are assigned for each subcomponent (i.e., stump, strut, brace, girder, and stem).

Additionally, the input should contain the effective length factor for buckling verification k_{buck} (default value=1), the unsupported length h_{twrb} (largest distance between consecutive flanges, e.g., 30 m), the z_{thoff} (distance from the tower-top flange to the hub center along z) and the material properties of the shell. The material density should be augmented for secondary steel and flanges, which are not directly accounted for, unless the discrete span input is selected. If the input Δz_{mx} (maximum FEA element length for the tower elements) is supplied, then $n_{div,twr}$ may be overridden to ensure that every tower element length is below Δz_{mx}. A minimum of two elements per segment is allowed.

Table 12. Variables and Parameters Used in the Definition of the Tower in JacketSE

Input[(a)]	Type	Description	Default Value	Units
D_b	variable	tower-base OD	5	m
DTR_b	variable	tower-base DTR	120	–
D_t	variable	tower-top OD	3	m
DTR_t	variable	tower-top DTR	120	–
h_{2f}	variable	fraction of tower length at constant cross section	0.25	–
h_{twr}	parameter	tower length	–	m
z_{hub}	parameter	hub height above MSL	–	m
z_{tb}	parameter	elevation MSL of tower-base	–	m
$n_{div,twr}$	parameter	number of elements in each of the two tower segments	$[4, 10]$	–
$\mathbf{CM_{off}}$	parameter	distance vector from the tower-top flange to the CM of the RNA	–	m
$\boldsymbol{\delta_{thoff}}$	parameter	distance vector from the tower-top flange to the hub center	–	m
ψ	parameter	rotor yaw angle about global z	45	°
h_{twrb}	parameter	tower buckling effective length, shortest distance between flanges	30	m
rig_{flg}	parameter	flag selecting how to treat the rigid connection at tower-top with the RNA	False	–
Δz_{mx}	parameter	maximum FEA element length for the tower elements	–	m
k_{buck}	parameter	buckling parameter or effective length factor	1	–
$\rho^{(b)}$	parameter	material density	7805	$\mathrm{kg\,m^{-3}}$
$E^{(b)}$	parameter	Young's modulus	2.1e11	$\mathrm{N\,m^{-2}}$
$G^{(b)}$	parameter	shear modulus	7.895e10	$\mathrm{N\,m^{-2}}$
$\nu^{(b)}$	parameter	Poisson's ratio	0.3	–
$f_y{}^{(b)}$	parameter	characteristic yield strength	345	$\mathrm{N\,m^{-2}}$

[a] Symbols used in this manual might differ from those used in the actual code, which are typeset from alphanumeric, standard-set characters, but they can be easily referred to the variable names in the current version of JacketSE. See https://github.com/WISDEM/JacketSE.git.
[b] Material properties can be either assigned for the entire tower or specifically for each member along the length of the tower.

If both h_{twr} and z_{hub} are provided, JacketSE will verify that the two values are compatible given z_{tb} and z_{thoff}, otherwise an error message is issued and the program quits. If z_{thoff} is not given or left at 0 m, it will be initialized at z_{cmoff} (distance from the tower-top flange to the RNA CM along z). Note that z_{tb} must coincide with the top node of the TP.

The tower is assumed rigidly connected to the RNA. This is represented either by a very stiff, massless FEA element (this is a legacy of older code and that will be discontinued in future versions), or it can be handled mathematically (preferred). In the latter case, the RNA inertia tensor elements (mass and six second moments referred to the CM (i.e., I_{xx},I_{yy},I_{zz},I_{xy},I_{yz}, and I_{xz}) and the $\mathbf{CM_{off}}$ (distance vector from the tower-top flange to the CM of the RNA) are directly input into the mass matrix of the FEA solver. The input switch rig_{flg} is a boolean input that instructs the code on how to treat the RNA connection. The presence of a $\psi \neq 0$ is also accounted for, by rotating the RNA inertia tensor accordingly.

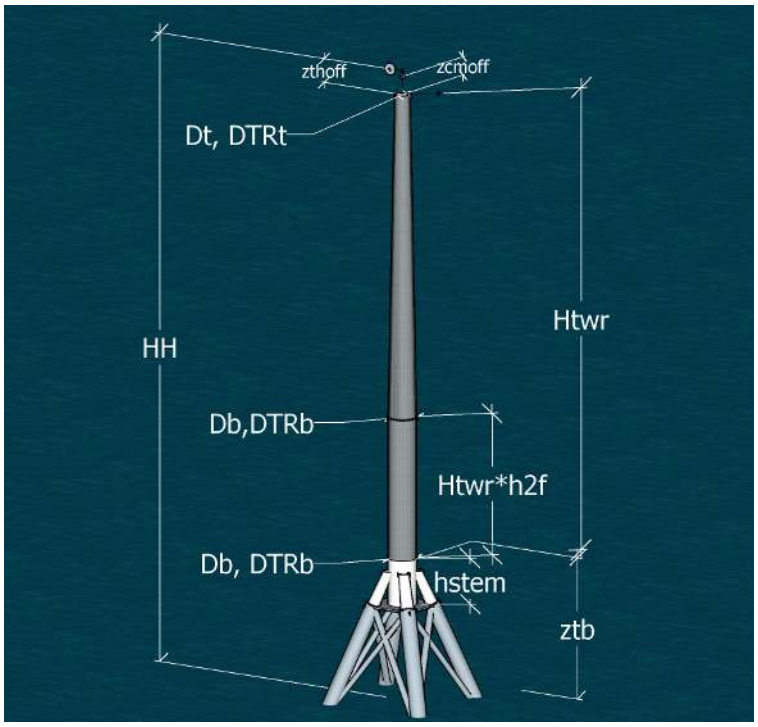

Figure 6. The main design variables and parameters for the tower model adopted by JacketSE

In place of D_b, DTR_b, D_t, DTR_t, h_{twr}, and h_{2f}, the tower may be defined by a set of discrete stations along the span, which are identified by triplets containing z coordinate values, ODs, and t's at the corresponding locations. The coordinates input in this fashion will be directly used as FEA nodes, and no further mesh refinement is needed. Concentrated, lumped masses can also be input in this case.

The resulting FEA elements are constant cross-section beam elements, thus, using an adequate number of elements $n_{div,twr}$ (or a proper span discretization) is recommended to accurately capture the taper of the tower. Tapered elements will be made available in a future release of the code.

The ψ is used to properly rotate the RNA inertia tensor and pass that information to the FEA solver. Additionally, $\boldsymbol{\delta_{\mathbf{thoff}}}$ (distance vector from the tower-top flange to the hub center) is also rotated by ψ so that RNA loads are placed correctly.

2.10 Loads

The loads that are considered by JacketSE can be categorized into permanent actions (dead loads) and live loads. Dead loads are the gravitational loads associated with the self-weight of the structure and secondary steel, such as tower internals, deck appurtenances (such as transformers and cranes), anodes, platforms, boat landings, and so on. Because of the vibrational and deflection characteristics of the OWT, even these so-called dead loads have very important dynamic effects—for example, the $P-\Delta$ effect associated with the displacement of the RNA *CM* (center of mass). Because JacketSE does not resolve these secondary and nonlinear effects, it is recommended that PSF and load estimation be selected conservatively. Furthermore, secondary steel can only be accounted for by concentrated masses at tower nodes and at the center of the TP deck. Applying a fictitious, increased steel density for the jacket and the tower may help simulate the effect of hardware, cathodic protection, and coatings.

The live loads considered by JacketSE include: aerodynamic loads from the RNA, i.e., forces $\mathbf{F_{aero}}$ and moments

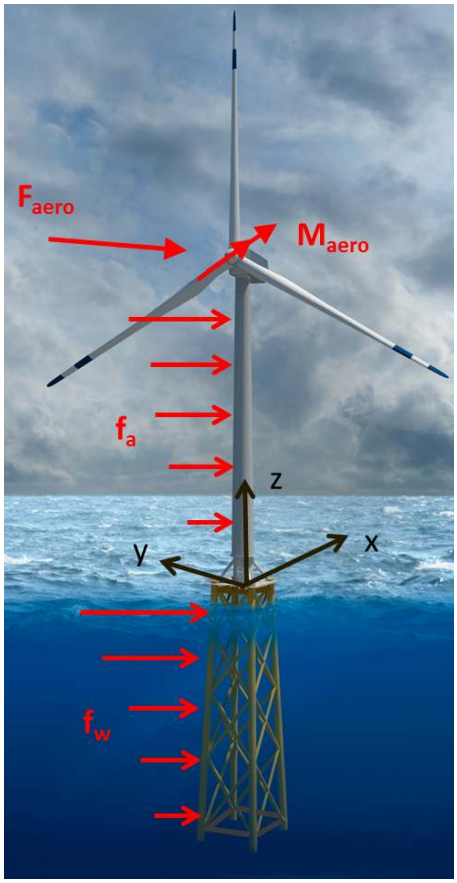

Figure 7. Main reference system used in JacketSE and principal sources of loading and their general areas of application. ***Original illustration by Joshua Bauer, NREL (modified here)***

$\mathbf{M_{aero}}$ originating at the rotor (augmented for dynamic amplification and vibrational effects); drag loads from direct action of the wind on the support structure; and hydrodynamic loads.

At this point in the development, other important sources of loads—e.g., installation loads, accidental loads, vortex-induced vibrations, ice, and seismic loadsDamiani (2016)—are ignored, and a number of simplifications in the calculation of live loads are employed, as discussed below.

In Figure 7, the approximate location of the loads' application points from the RNA and hydrodynamics is shown together with the main coordinate system adopted by JacketSE.

The primary simplification in JacketSE is the treatment of all loads as pseudo-static. This approximation reduces computational time and resources, whereas an accurate determination of dynamic load components demands sophisticated computer-aided engineering (CAE) tools and coupled numerical simulations. Thus, users must exercise care in selecting loads and PSFs to compensate for the lack of a fully dynamic treatment. Furthermore, FLS verification is not directly performed, which is a capability that will be implemented in future versions of JacketSE. In general, fatigue loading tends to dominate the design of the flanges and welds for the tower, and the joints of the jacket, whereas the main shells are driven by modal and buckling-strength requirements.

The primary loading source for the tower comes from the aerodynamic loads induced by the rotor. The substructure must resist the combination of RNA loads and hydrodynamics loads, with the latter becoming more and more important as water depth and wave heights increase.

Tower shear and bending moments from the direct wind action on the tower, as well as wave and current loads on the jacket legs, are approximated following basic fluid-dynamics principles. Through consultations of the standards, wind shear values (IEC 2009) and δ_fs—or gust factors from DIN (2005), European Committee for Standardisation (2010), and SEI (2005, 2010)—may be obtained to calculate and integrate the drag force along the tower span.

The default set-up for JacketSE allows for two main DLCs, usually taken as:

1. An operational DLC, similar to DLC 1.6 from IEC (2009)
2. A parked DLC, similar to DLC 6.1 from IEC (2009).

For these two cases, loads and environmental conditions can be input independently. Additional load cases can be coded into the program relatively easily.

Some of the additional parameters needed to define the loads in JacketSE are given in Table 13, with more details presented in the following Sections. More details about the load calculations are given in the Sections 2.10.1–2.10.4.

2.10.1 RNA Loads

From a quasi-steady-state point of view, the RNA loads reduce to three forces and three moments along the main coordinate axes—see Damiani (2016) for more details on load sources. These loads are generated by the rotor aerodynamics in a turbulent and sheared inflow under tower interference effects and structural imbalance. In addition to the normal operating loads, transients such as shutdowns, and blade/rotor/yaw faults can give rise to important ULS loads for the support structure and should not be underestimated. Other important load contributions derive from the gyroscopic effects when the turbine yaws with the rotor spinning.

The thrust is the biggest force responsible for the bending moment distribution along the tower and loads on the sub-structure. For a downwind turbine, the additional effect of the gravitational load caused by a downwind offset of the RNA *CM* from the tower centerline may significantly increase the tower utilization. In an upwind turbine, the RNA mass contribution to the bending moment is minimal and any upwind offset of the RNA *CM* can be conservatively ignored, as the $P-\Delta$ effect would tend to reduce that contribution anyway.

From a FLS standpoint, the aerodynamic loads associated with the RNA tend to dominate the design, with the exception of cases in deep water sites where hydrodynamics excitation and low damping situations can also be important.

Various methods exist to estimate RNA loads, and they are not discussed in this manual—for more details, see Damiani (2016). JacketSE assumes that the input RNA loads account for dynamic amplification, such as those that may be derived from aero-elastic analyses.

2.10.2 Aerodynamic Loading

Direct wind loading on the tower and jacket is caused by aerodynamic drag on the structural elements. The wind profile can be taken as in Eq. (2.37), where α (wind power law exponent) is given by the standards—e.g., IEC (2009)—and as input to JacketSE.

$$|\mathbf{U}(z)| = |\mathbf{U_{hub}}| \left(\frac{z}{z_{hub}}\right)^{\alpha} \tag{2.37}$$

where $\mathbf{U}(z)$ is the wind velocity vector as a function of z, the altitude above MSL, and $\mathbf{U_{hub}}$ is the wind velocity at hub height (i.e., z_{hub}).

For a typical tubular member of the tower or jacket, Eq. (2.38) can be used to calculate the pseudo-static loads on the tower due to wind action on its cylindrical or conical segments.

$$\mathbf{f_a} = 0.5\rho_a \pi D_{sh} c_d G_f \mathbf{U}|\mathbf{U}| \tag{2.38}$$

Table 13. Additional Parameters Used in the Definition of the Loads in JacketSE

Input[(a)]	Type	Description	Default Value	Units
$\mathbf{F_{aero}}$	variable	force vector originating at the rotor	–	N
$\mathbf{M_{aero}}$	variable	moment vector originating at the rotor	–	N m
$\mathbf{CM_{off}}$	parameter	distance vector from the tower-top flange to the *CM* of the RNA	–	m
$\boldsymbol{\delta_{thoff}}$	parameter	distance vector from the tower-top flange to the hub center	–	m
ψ	parameter	rotor yaw angle about global z	45	°
$\mathbf{U_{hub}}$	parameter	wind velocity at hub height	–	$\mathrm{m\,s^{-1}}$
α	parameter	wind power law exponent	0.2	–
h_w	parameter	maximum (e.g., 50 yr) wave height(s) under operation and parked conditions	–	m
T_w	parameter	maximum (e.g., 50 yr) wave nominal period under operation and parked conditions	–	s
$\mathbf{u_c}$	parameter	current velocity	–	$\mathrm{m\,s^{-1}}$
ρ_a	parameter	air density	1.225	$\mathrm{kg\,m^{-3}}$
ρ_w	parameter	sea water density	1025	$\mathrm{kg\,m^{-3}}$
G_f	parameter	gust factor	–	–
$c_{d,at}$	parameter	air drag coefficient tower	–	–
$c_{d,aj}$	parameter	air drag coefficient jacket	–	–
c_m	parameter	added mass coefficient	–	–
$c_{d,wj}$	parameter	water drag coefficient jacket	–	–
γ_f	parameter	generic load PSF	1.35	–
γ_{fg}	parameter	gravitational load PSF	1.1	–
γ_{fa}	parameter	aerodynamic load PSF	1.35	–
γ_m	parameter	material PSF	1.	–
γ_n	parameter	consequence of failure PSF	1.	–

[a] Symbols used in this manual might differ from those used in the actual code, which are typeset from alphanumeric, standard-set characters, but they can be easily referred to the variable names in the current version of JacketSE. See https://github.com/WISDEM/JacketSE.git.

where $\mathbf{f_a}$ is the force per unit length caused by wind aerodynamic drag, ρ_a is the air density, D_{sh} is the OD of the tower or jacket leg member, c_d is the air drag coefficient (e.g., $\simeq 0.6 - 0.7$ for tower segments), and G_f is the gust factor; all are potentially functions of the height above MSL.

JacketSE integrates Eq. (2.38) along the span of the tower, adds the thrust and moments from the RNA, and calculates the total shears and bending moments along the tower segments. Normally, the thrust of the rotor under operational DLCs is by far the dominant contributor to the bending stresses in the tower shell, and for FLS verification the direct wind drag is less important; but parked cases under ULS conditions may give rise to important drag loads that cannot be underestimated especially for high hub heights and smaller rotors.

The gust factor in Eq. (2.38) accounts for the effect on wind actions from the nonsimultaneous occurrence of peak wind pressures on the structure surface together with the effect of the vibrations of the structure caused by turbulence. Various methods to calculate G_f are offered by the standards—e.g., DIN (2005), European Committee for

Standardisation (2010), and SEI (2005, 2010)—, and more recent treatments with focus on wind turbine towers can be found in Burton et al. (2005) and Murtagh, Basu, and Broderick (2007). Per SEI (2005), structures are defined as dynamically sensitive (or flexible) if their first natural frequency is $f_0 < 1\,\text{Hz}$—more detailed criteria can be found in European Committee for Standardisation (2010) Part 1-4. When this criterion is met, G_f can be significantly larger than one.

JacketSE requires the c_d input value to account for G_f. Furthermore, two values can be input: one for the jacket ($c_{d,aj}$) and one for the tower ($c_{d,at}$). The aerodynamic drag is, in fact, computed also on the jacket leg members above MSL following Eq. (2.38), where D_{sh} is replaced by D_{leg}. Because of the leg three-dimensional orientation, the component of $\mathbf{U}$ normal to the leg is considered in Eq. (2.38) and the resulting force is further decomposed into a horizontal and a vertical force. Because no aerodynamic force is computed for the cross members and the TP, the $c_{d,at}$ and $c_{d,aj}$ should be augmented to account for the load contributions from these members.

2.10.3 Hydrodynamic Loading

The effects of wave and current kinematics on the loading of a jacket can be calculated via the Morison equation for slender members:

$$\mathbf{f_w} = 0.25\rho_w \pi D_{leg}^2 c_m \dot{\mathbf{U}}_\mathbf{w} + 0.5\rho_w \pi D_{leg} c_{d,wj} \mathbf{U_w}|\mathbf{U_w}| \tag{2.39}$$

where $\mathbf{f_w}$ is the force per unit length as a result of wave and current kinematics, ρ_w is the sea water density, $\mathbf{U_w}$=$\mathbf{u_w}$+$\mathbf{u_c}$ is the vectorial sum of the wave and current velocity (vector sum), and $c_{d,wj}$ and c_m are the water drag coefficient jacket and the added mass coefficient, respectively.

The coefficients $c_{d,wj}$ and c_m should account for the presence of marine growth, and depend on Reynolds and Keulegan-Carpenter numbers, thus on the specific DLC under consideration—see also ISO (2014).

JacketSE assumes a uniform (unsheared) current velocity aligned with the wave direction. The wave particle-kinematic velocity is calculated via Airy theory—see Eq. (2.40), ISO (2014). This theory does not account for any stretching, therefore the loads calculated through Eqs. (2.39)-(2.40) may be underestimated.

$$\begin{aligned} \mathbf{u_w} &= h_w \omega_w \frac{\cosh \kappa_w (d_w + z_w)}{\sinh \kappa_w d_w} \\ \dot{\mathbf{u}}_\mathbf{w} &= h_w \omega_w^2 \frac{\sinh \kappa_w (d_w + z_w)}{\sinh \kappa_w d_w} \cos(\kappa_w x - \omega_w t_t) \end{aligned} \tag{2.40}$$

In Equation (2.40), h_w is the wave height, (peak-to-peak distance), z_w is the distance from the sea surface, positive upwards, κ_w is the wave number, ω_w is the wave frequency, x is the wave propagation direction, and t_t is the time variable. Two further simplifications are adopted in JacketSE. First, the hydrodynamic loads are solely calculated on the main leg members, ignoring the direct contribution to the wave and current forces from the cross members. Second, the maximum wave speed and acceleration are conservatively considered as acting simultaneously, thus ignoring any phase effect and essentially dropping the time dependency, while also not including any structural motion.

To account for additional loads on the cross-braces and the absence of wave stretching, applying larger-than-normal hydrodynamic coefficients is recommended. The conservatism associated with the static treatment of the wave kinematics helps further mitigate the consequences of a cursory treatment of the hydrodynamics.

In the literature, corrections to the Morison equation have been proposed for diffraction effects—e.g., the MacCamy-Fuchs correction, Chakrabarti (1987)—, and for wave nonlinearities. In addition, the probability of breaking wave occurrence (normally when $h_w/d_w > 0.78$) and associated slamming loads (DNV 2013) on the support structures (SSts) should be verified, because these loads are not directly included in JacketSE.

In real structures, other concentrated loads may derive from the presence of boat landings and J-tubes, which may attract more wave loads not accounted by JacketSE. These loads are normally less impactful, yet the welded connections to the principal steel may be a source of crack nucleation and corrosion.

Because all of these aspects could be important, we again recommend using conservative estimates for $c_{d,wj}$ and c_m and PSFs. Future releases will refine the hydrodynamics loading model to overcome the limitations of this simplified treatment.

2.10.4 Loads Integration

Analytically, the various contributions to the tower internal loads could be accounted for as in Eqs. (2.41)-(2.44). The normal (axial, along the z axis) force can be written as:

$$N_d(z) = \gamma_f F_{z_{RNA}} - \gamma_{fg} m_{RNA} g - \gamma_{fg} \int_z^L \rho A g dz \tag{2.41}$$

where N_d is the design (factored) normal load at the tower station of interest, $F_{z_{RNA}}$ is the aerodynamic force from the RNA along the z axis, γ_f is the generic load PSF, m_{RNA} is the RNA mass, g is the gravity acceleration, γ_{fg} is the gravitational load PSF, ρ is the material density, L is the generic member length, A is the member cross-sectional area, and z is the z coordinate along the tower span. The last two of the three terms on the right-hand side of Eq. (2.41) are automatically calculated by the FEA solver (see Section 2.11), whereas the first term is part of the input to JacketSE.

The shear components along x and y (reference system is that of Figure 7) can be calculated as:

$$T_x(z) = \gamma_f F_{x_{RNA}} + \gamma_{fa} \int_z^L \mathbf{f_a} \cdot \hat{i} d\zeta \tag{2.42a}$$

$$T_y(z) = \gamma_f F_{y_{RNA}} + \gamma_{fa} \int_z^L \mathbf{f_a} \cdot \hat{j} d\zeta \tag{2.42b}$$

where $F_{x_{RNA}}$ is the force from the RNA along the x-axis, $F_{y_{RNA}}$ is the force from the RNA along the y-axis, $\mathbf{f_a}$ is given in Eq. (2.38), γ_{fa} is the aerodynamic load PSF, $\hat{i}$ is the unit vector along the x-axis, $\hat{j}$ is the unit vector along the y-axis, and ζ is the dummy coordinate along the z-axis. Whereas $F_{x_{RNA}}$ and $F_{y_{RNA}}$ are inputs to JacketSE, the integrals in Eq. (2.42) are replaced by a two-step approach. First, a discrete integration of the distributed wind pressure over the tower elements is performed and equivalent shear loads are applied at the element nodes. Second, during utilization calculation, these forces are numerically integrated via simple quadrature to obtain the actual internal shear loads.

The bending moment components can be written as follows:

$$M_x(z) = \gamma_f \;\; M_{x_{RNA}} - F_{y_{RNA}}(z_{RNA} - z) \;\; - \int_z^L \;\; \gamma_{fa} \mathbf{f_a} \cdot \hat{j}\zeta + \gamma_{fg} \rho A g (y(\zeta) - y(z)) \;\; d\zeta \tag{2.43a}$$

$$M_y(z) = \gamma_f \;\; M_{y_{RNA}} + F_{x_{RNA}}(z_{RNA} - z) \;\; + \int_z^L \;\; \gamma_{fa} \mathbf{f_a} \cdot \hat{i}\zeta + \gamma_{fg} \rho A g (x(\zeta) - x(z)) \;\; d\zeta \tag{2.43b}$$

where M_x is the component of the bending moment along the x-axis at the station of interest, M_y is the component of the bending moment load along the y-axis at the station of interest, $M_{x_{RNA}}$ is the RNA aerodynamic moment along the x-axis, $M_{y_{RNA}}$ is the RNA aerodynamic moment along the y-axis, $\rho A g$ is the distributed mass in $\mathrm{kg\,m^{-1}}$, and $(x(\zeta) - x(z))$ and $(y(\zeta) - y(z))$ account for the deflection of the tower axis along x and y from the undeflected position. JacketSE, however, does not account for second order $P - \Delta$ effects, so the second terms within the integrals are ignored. The remainder terms within the integrals are again replaced by a simple numerical quadrature of the distributed pressure over the span of the tower, and bending moment values are applied at the element nodes. Potentially different PSFs for the various loading components can be employed following standards such as Germanischer Lloyd (2005) and input into JacketSE. Finally, the torque about the z-axis is given by:

$$M_z(z) = \gamma_f \;\; M_{z_{RNA}} - F_{x_{RNA}} \left(y(z_{RNA}) - y(z)\right) + F_{y_{RNA}} \left(x(z_{RNA}) - x(z)\right) \tag{2.44}$$

where M_z is the torsion moment load along the z-axis at the station of interest. Note no further contribution to torque along the tower axis is considered.

The shear and moment components can then be combined to arrive at characteristic design values:

$$T_d(z) = \sqrt{T_x(z)^2 + T_y(z)^2} \tag{2.45a}$$

$$M_d(z) = \sqrt{M_x(z)^2 + M_y(z)^2} \tag{2.45b}$$

Note that for the tower, the internal loads are calculated externally to the FEA solver (pyFrame3DD) while separating contributions from gravity loads and aerodynamics, but these loads could just as well be calculated by pyFrame3DD.

For the jacket leg (and any exposed portion of the piling), wind and hydrodynamic loads are computed numerically by integrating Eq. (2.39) below the water surface and Eq. (2.38) above the water line, and then by applying equivalent concentrated forces at the leg nodes, as per Eq. (2.46):

$$T_x(z_i) = \gamma_{fw} \int_{z_i}^{L} \mathbf{f_w} \cdot \hat{\imath} d\zeta \tag{2.46a}$$

$$T_y(z_i) = \gamma_{fa} \int_{z_i}^{L} \mathbf{f_a} \cdot \hat{\jmath} d\zeta \tag{2.46b}$$

where γ_{fw} is the hydrodynamic load PSF.

The internal loads are calculated by pyFrame3DD and used for utilization verification.

Rotation matrices are employed to account for batter in the legs and rotor yaw alignment. The DLCs discussed in Section 2.10 consider wind and wave along the main diagonal of a four-legged jacket. In that case, the shear from air and water drag on upstream and downstream legs generate both shear and tensile (compression) forces that are given by the decomposition of wave forces assumed normal to the legs' axes. For the sake of simplicity, the air drag is also considered normal to the leg axis, which is more conservative, as most of the load goes into bending. For the other two legs, the load is considered horizontal (i.e., normal to the vertical plane that contains them).

The internal loads are then used to derive stresses and calculate the utilization in both tower and jacket members and joints as discussed below.

Although the above treatment is sufficient for conceptual and preliminary assessments, only rigorous loads and FEA analyses can fully support a more detailed design. In particular, fully coupled loads analyses via aero-hydro-servo-elastic (AHSE) simulations are the only way to capture important interactions and vibrational dynamics and to perform FLS and ULS verifications for the certification of OWTs' support structures.

The FLS verification will be implemented in future releases of the software.

2.11 FEA Solver

The FEA solver at the core of JacketSE is based on a modified version of FRAME3DD. FRAME3DD is an open-source software for static and dynamic structural analysis of two- and three-dimensional beam frames and trusses with elastic and geometric stiffness. It computes the static deflections, reactions, internal element forces, natural frequencies, mode shapes, and modal participation factors of two- and three-dimensional elastic structures using direct stiffness and mass assembly. The theory is based on a Timoshenko beam element—see Timoshenko (1970) and Panzer et al. (2009)—and the source code is in C. A python module called *pyframe3DD* (see https://github.com/WISDEM/pyFrame3DD) was developed to run FRAME3DD without the need for input and output files. pyFrame3DD runs seamlessly with the JacketSE, and optional inputs for FRAME3DD are handled via JacketSE's inputs (see Table 14).

Furthermore, pyFrame3DD accepts arbitrary stiffness values at constraint nodes (rather than only rigid or free). This allows for the soil-pile interaction stiffness to be incorporated into the JacketSE model, as discussed in Section 2.3.2.

Table 14. Input Parameters for FRAME3DD Handled by JacketSE's Inputs—For More Details See Gavin (2010)

Parameter	Type	Description	Default Value
sh_{fg}	Boolean switch	0/1 = do not/do include shear deformation effects	1
Δ_z	Floating point (m)	Step size along member axis for internal load calculations	-1 (ignore) [a]
gm_{fg}	Boolean switch	0/1 = do not/do include geometric stiffness effects	0
$\vec{g}$	Three-element floating point array	Inertial frame acceleration	$[0, 0, -9.81]$
n_{mod}	Integer	Number of eigenvalues/eigenmodes to calculate	6
M_{mod}	Integer switch	Dynamic eigenvalue method: 1 = subspace-Jacobi iteration; 2 = Stodola (matrix iteration)	1
l_m	Integer switch	Mass modeling method: 0 = consistent mass matrix; 1 = lumped mass matrix	0
δ_{shf}	Floating point	Frequency shift factor for rigid-body modes in case of partially restrained structure	0
R_{dx}	Integer switch	Matrix condensation method: 0 = none; 1 = static; 2 = Guyan; 3 = dynamic	2

[a] Internal forces are calculated at element nodes, i.e., more than one element ($n_{div} > 1$) is recommended with the current version of JacketSE.

Table 15. Examples of ULS, SLS, and FLS Load PSFs—From IEC 2005

Limit State	Unfavorable Loads			Favorable Loads
	Normal[a]	Abnormal	Transport and Installation	All DLCs
ULS/SLS	1.35	1.1	1.5	0.9
FLS	1.0	1.0	1.0	1.0

[a] Normal or abnormal attributes for the various DLCs are given by the standards—e.g., IEC (2009).

pyFrame3DD also allows for lumped masses to be distributed at model nodes (for instance, to simulate TP or RNA inertia) affecting both modal and static load response.

Whereas FRAME3DD is capable of directly using linear and trapezoidal external force distributions along the elements, and of calculating element internal forces, the current versions of JacketSE solely relies on nodal forces. The load module condenses the distributed pressure loads from wind and waves at element nodes, and the verifications are performed at the node level. As a result, it is important to have enough resolution to resolve the pressure loads. Future versions will take advantage of element internal load calculations and relax the need for higher element resolution.

2.12 Utilization Calculation

2.12.1 Safety Factors

The generic ULS limit state verification may be expressed as follows (IEC 2005):

$$\gamma_n S(F_d) \leq R(f_d) \tag{2.47a}$$

$$\text{or} \quad \text{explicitly} \tag{2.47b}$$

$$\gamma_f F_k \leq \frac{f_k}{\gamma_n \gamma_m} \tag{2.47c}$$

where $S(F_d)$ is the probability distribution of the generic, design (factored) load within the Load Resistance Factor Design approach, $R(f_d)$ is the analogous function for the material-factored resistance, F_d (F_k) is the factored (unfactored) characteristic load, f_d (f_k) is the material-factored (unfactored) resistance, γ_n is the consequence of failure PSF (or 'importance' factor based on the redundancy and fail-safe characteristics of the various components), γ_f is the generic load PSF, and γ_m is the material PSF.

The intent of JacketSE is not to deliver a final design, but to inspect the impact of various design choices under some key DLCs from different perspectives, including LCOE aspects, as mentioned in Section 1. More accurate AHSE loads analyses and subcomponent FEAs are needed to arrive at a detailed design. Design standards provide guidance for determining characteristic loads through AHSE loads analyses (Germanischer Lloyd 2012; IEC 2005). Furthermore, the standards provide recommended values for γ_f and γ_n (see also Tables 15–16) (IEC 2009, 2005; Germanischer Lloyd 2012; DNV 2013; ISO 2007; API 2014). These PSFs represent the uncertainty in the load stochastic distribution and in the load assessment, and can be input to JacketSE. Material PSFs can be either taken from specific, recognized design codes—e.g., ANSI (2010), European Committee for Standardisation (2005), ABS (2014), and DNV (2010)—, or alternatively their minimum values may be taken as in Table 17 from IEC (2005).

Note that, per AWEA (2012), the OWT and its components should satisfy the 'L2' exposure category (API 2014), which also requires that a 500 yr robustness check be carried out with unity PSFs. This check could be accomplished by setting appropriate unit PSFs and environmental conditions as inputs into JacketSE; however, given the levels of approximation in JacketSE, higher than normal PSFs are recommended.

Table 16. Examples of Minimum γ_n As a Function of Component Class—From IEC (2005)

Component Class	γ_n			Comment
	ULS	FLS	SLS	
1	0.9	1.0	1.0	'Fail-safe' structural components whose failures do not result in the failure of a major part of a wind turbine (e.g., replaceable bearings)
2	1.0	1.15	1.0	'Nonfail-safe' structural components whose failures may lead to the failure of a major part of a wind turbine
3	1.3	1.3	1.3	'Nonfail-safe' mechanical components that link actuators and brakes to main structural components for the purpose of implementing nonredundant turbine protection functions

Table 17. Examples of Minimum γ_m As a Function of Failure Mode—From IEC (2005)

Failure Mode	γ_m		
	ULS	FLS	SLS
Yielding of ductile materials	1.1	1.1 (welded and structural steel) to 1.7 (composites)	1.0 (if elastic properties proven by full-scale testing); 1.1 (otherwise)
Global buckling of curved shells	1.2		
Rupture from exceeding tensile or compression strength	1.3		

JacketSE recasts Eq. (2.47c) in utilization equations for the tower and the substructure. Although the utilization checks should be performed for FLS, SLS, and ULS, the current version of JacketSE only performs ULS and SLS verifications.

ULS structural checks ensure that the material utilization is below one, and that deflections are below limits specified by the user. The verification is conducted on steel members under tension and compression-bending and following the main standards of reference.

2.12.2 Tower Utilization

The normal stresses ($\sigma_{z,Ed}$ along the meridional and $\sigma_{\theta,Ed}$ along the circumferential directions), the shear stress ($\tau_{z\theta,Ed}$), and the von-Mises equivalent stress (σ_{vm}) for the generic cross section of the tubular tower can conservatively be written as:

$$\sigma_{z,Ed} = \frac{N_d}{A} + \frac{M_d D_{sh}}{2J_{xx}} \tag{2.48a}$$

$$\sigma_{\theta,Ed} = \gamma_f (k_w - 1) q_{max} \frac{D_{sh} - t_{sh}}{2t_{sh}} \tag{2.48b}$$

$$\tau_{z\theta,Ed} = 2T_d/A + \frac{M_z}{2A_{mid} t_{sh}} \tag{2.48c}$$

$$\sigma_{vm} = \sqrt{\sigma_{z,Ed}^2 + \sigma_{\theta,Ed}^2 - \sigma_{z,Ed}\sigma_{\theta,Ed} + 3\tau_{z\theta,Ed}^2} \tag{2.48d}$$

where the argument z was dropped without losing generality, k_w is the dynamic pressure factor to calculate hoop stresses function of cylinder dimensions and external pressure buckling factor per European Committee for Standardisation (1993), t_{sh} is the shell t, A_{mid} is the area inscribed by the midthickness line, and all the other symbols were introduced earlier except for q_{max}, which is the maximum wind dynamic pressure expressed as in Eq. (2.49):

$$q_{max} = 0.5 * \rho_a |\mathbf{U}|^2 \tag{2.49}$$

The tower can be considered verified if, for all of the segments, it can be proved that the stresses are kept below the allowable yield strength, and stability is guaranteed at a global and local level. These constraints can be expressed by the following equations (Germanischer Lloyd 2005; European Committee for Standardisation 1993):

$$\sigma_{vm} \leq \frac{f_y}{\gamma_m \gamma_n} \tag{2.50}$$

$$\frac{N_d}{\kappa N_p} + \frac{\beta_m M_d}{M_p} + \Delta_n \leq 1 \tag{2.51}$$

$$\sigma_{z,Ed} \leq \sigma_{z,Rd} \tag{2.52a}$$

$$\sigma_{\theta,Ed} \leq \sigma_{\theta,Rd} \tag{2.52b}$$

$$\tau_{z\theta,Ed} \leq \tau_{z\theta,Rd} \tag{2.52c}$$

$$\left(\frac{\sigma_{z,Ed}}{\sigma_{z,Rd}}\right)^{k_z} + \left(\frac{\sigma_{\theta,Ed}}{\sigma_{\theta,Rd}}\right)^{k_\theta} - \frac{\sigma_{z,Ed}\sigma_{\theta,Ed}}{\sigma_{z,Rd}\sigma_{\theta,Rd}} k_i + \left(\frac{\tau_{z\theta,Ed}}{\tau_{z\theta,Rd}}\right)^{k_\tau} \leq 1 \tag{2.52d}$$

Eq. (2.50) states the constraint on the yield resistance of the material (f_y).

Eq. (2.51) is the global (Eulerian) buckling constraint, where N_d and M_d are the design axial and bending moment loads, as calculated by the load module (see Section 2.10.4), N_p and M_p are the characteristic, buckling-critical, resistance values, κ and β_m are reduction factors for the flexural buckling and bending moment coefficient, respectively

(Germanischer Lloyd 2005), and Δ_n is a function of the slenderness ($\bar{\lambda}$) of the tower as in Eq. (2.53):

$$\begin{aligned} \Delta_n &= 0.25\kappa\bar{\lambda}^2 \\ \bar{\lambda} &= \sqrt{\frac{N_p\gamma_m}{N_e}} \end{aligned} \tag{2.53}$$

κ is given by:

$$\begin{aligned} \kappa = & \quad \frac{1}{\Phi+\sqrt{\Phi^2+\bar{\lambda}^2}} \leq 1 \quad \text{for } \bar{\lambda} > 0.2 \\ & \quad 1 \qquad\qquad\qquad\quad \text{for } \bar{\lambda} \leq 0.2 \\ \text{with:} & \\ \Phi = 0.5 & \ 1+\alpha_b \ \bar{\lambda}-0.2 \ +\bar{\lambda}^2 \end{aligned} \tag{2.54}$$

α_b is the imperfection factor used in the buckling calculation, set equal to 0.21 in JacketSE. The elastic buckling resistance N_e is taken as:

$$N_e = \frac{\pi^2 E J_{xx}}{1.1 s_k} \tag{2.55}$$

where s_k is the buckling length factor, set equal to 2 for the tower in JacketSE, E is the Young's modulus, J_{xx} is the member cross-sectional, second area-moment of inertia. The buckling resistance values are taken as in Eq. (2.56):

$$N_p = A\frac{f_y}{\gamma_b} \tag{2.56a}$$

$$M_p = W_p\frac{f_y}{\gamma_b} \tag{2.56b}$$

where W_p is the cross-sectional bending modulus, and γ_b is the safety factor used in buckling verification, usually set equal to 1.1 (Germanischer Lloyd 2005).

Eq. (2.52) is the local (shell) buckling constraint; $\sigma_{z,Ed}$, $\sigma_{\theta,Ed}$, and $\tau_{z\theta,Ed}$ are the design values of the axial, hoop, and shear stress, respectively, $\sigma_{z,Rd}$, $\sigma_{\theta,Rd}$, and $\tau_{z\theta,Rd}$ are the corresponding characteristic buckling strengths, k_z, k_θ, k_τ, and k_i are constants given by the standards (European Committee for Standardisation 1993). The buckling strengths are given by:

$$\begin{aligned} \sigma_{z,Rd} &= \frac{\chi_z f_y}{\gamma_m} \\ \sigma_{\theta,Rd} &= \frac{\chi_\theta f_y}{\gamma_m} \\ \tau_{z\theta,Rd} &= \frac{\chi_\theta f_y}{\sqrt{3}\gamma_m} \end{aligned} \tag{2.57}$$

where the generic buckling reduction factor in the shell buckling verification (χ) is given by:

$$\begin{aligned} \chi = & \begin{cases} 1 & \text{for} \quad \hat{\lambda} \leq \hat{\lambda}_0 \\ 1-\beta_p\left(\frac{\hat{\lambda}-\hat{\lambda}_0}{\hat{\lambda}_p-\hat{\lambda}_0}\right)^\eta & \text{for} \quad \hat{\lambda}_0 < \hat{\lambda} \leq \hat{\lambda}_p \\ \frac{\alpha_{imp}}{\hat{\lambda}^2} & \text{for} \quad \hat{\lambda}_p \leq \hat{\lambda} \end{cases} \\ \text{with} \quad \hat{\lambda}_p = & \sqrt{\frac{\alpha_{imp}}{1-\beta_p}} \end{aligned} \tag{2.58}$$

and the characteristic values for $\hat{\lambda}_0$, β_p, and η are shown in Table 18. In the table, the expressions of $\hat{\lambda}$ are given as

functions of $\sigma_{z,Rcr}$, $\sigma_{\theta,Rcr}$, and $\tau_{z\theta,Rcr}$, i.e., the critical buckling stresses shown in Eq. (2.59):

$$\sigma_{z,Rcr} = 0.605E\frac{C_z}{rtr} \tag{2.59a}$$

$$\sigma_{\theta,Rcr} = \begin{cases} 0.92E\frac{C_{\theta,s}}{\omega_b rtr} & \text{for } \frac{\omega_b}{C_\theta} < 20 \\ 0.92E\frac{C_\theta}{\omega_b rtr} & \text{for } 20 \le \frac{\omega_b}{C_\theta} \le 1.63rtr \\ \frac{E}{rtr^2}\ 0.275 + 2.03\ \left(\frac{C_\theta}{\omega_b}rtr\right)^4 & \text{for } \frac{\omega_b}{C_\theta} > 1.63rtr \end{cases} \tag{2.59b}$$

$$\tau_{z\theta,Rcr} = 0.75EC_\tau\frac{1}{\sqrt{\omega_b}rtr} \tag{2.59c}$$

where ω_b is the dimensionless length parameter for shell buckling calculations, rtr is the ratio of r_{eq} to t_{eq}, and the factors C_z, C_θ, $C_{\theta,s}$, and C_τ are shown in Eq. (2.60):

$$\omega_b = \frac{2L}{D}\sqrt{rtr} \tag{2.60a}$$

$$C_z = \begin{cases} 1.36 - \frac{1.83}{\omega_b} + \frac{2.07}{\omega_b^2} & \text{for } \omega_b < 1.7 \\ 1 & \text{for } 1.7 \le \omega_b \le 0.5rtr \\ \max\ 0.6, 1 + \frac{0.2}{6}\ 1 - \frac{2\omega_b}{rtr} & \text{for } \omega_b > 0.5rtr \end{cases} \tag{2.60b}$$

$$C_\theta = 1.5 \quad \text{assuming clamped-clamped boundary conditions} \tag{2.60c}$$

$$C_\tau = \begin{cases} \sqrt{1 + \frac{42}{\omega_b^3}} & \text{for } \omega_b < 10 \\ 1 & \text{for } 10 \le \omega_b \le 8.7rtr \\ \frac{1}{3}\ \sqrt{\frac{\omega_b}{rtr}} & \text{for } \omega_b > 8.7rtr \end{cases} \tag{2.60d}$$

The values for α_{imp} to be used in Eq. (2.58) are also given in Table 18, as a function of meridional compression fabrication quality parameter European Committee for Standardisation 1993 (Q) and the ratio of r_{eq} to t_{eq} (rtr). JacketSE assumes Q=25, i.e., class 'B' fabrication tolerance, and calculates rtr as:

$$rtr = \frac{r_{eq}}{t_{eq}\cos\beta_c} = \frac{D_2 + D_1}{4\,(t_2 + t_1)\cos\beta_c} \quad \text{with } \beta_c = \arctan\frac{D_2 - D_1}{2h_c} \tag{2.61}$$

where r_{eq} and t_{eq} are the equivalent OR and t for a tapered member (a segment of the tower shell), taken as the average OR and t, β_c is the cone angle for the typical tapered shell element, and h_c is the height of a tapered shell member.

JacketSE returns the left-hand side of Eqs. (2.50), (2.51), and (2.52) as utilization values.

In addition to FLS and ULS checks, an important structural check for both blade and tower design is the verification of potential blade strike on the tower, which is part of the SLS checks. Blade maximum deflection may occur under a transient event as in the case of extreme gusts or fault situations. In order to verify that a safety margin remains in the deflection of the blade before the tower strike, the maximum deflection across all ULS DLCs must be determined. Standards such as IEC (2005) and Germanischer Lloyd (2012) offer guidance on the PSFs to employ in this calculation: IEC (2005) uses the same load PSF as for any other ULS DLC, whereas Germanischer Lloyd (2012) states that the blade clearance shall not be less than 30% of the value under unloaded (at rest) conditions. JacketSE can return the deflection at the top of the tower and that combined with the blade deflection can be used to check for this SLS criteria.

Table 18. Values for $\hat{\lambda}_0$,η, and β_p As a Function of Stress Type—From European Committee for Standardisation (1993)

Stress Type	$\hat{\lambda}$	$\hat{\lambda}_0$	β_p	η	α_{imp}
Axial	$\sqrt{\frac{f_y}{\sigma_{z,Rcr}}}$	0.2	0.6	1	$\frac{0.62}{1+1.91(\Delta w_k/t)^{1.44}}$ [a]
Hoop	$\sqrt{\frac{f_y}{\sigma_{\theta,Rcr}}}$	0.4	0.6	1	0.65
Shear	$\sqrt{\frac{f_y}{\sqrt{3}\tau_{z\theta,Rcr}}}$	0.4	0.6	1	

[a] Δw_k is the characteristic imperfection amplitude European Committee for Standardisation 1993, $\Delta w_k = \frac{1}{Q}\sqrt{rtr}$.

2.12.3 Jacket Utilization

The substructure utilization is calculated at the joints and members per API (2014). For simplicity, all the joints between two cross-braces are considered as x-joints, and all of the joints involving a brace and a leg are considered as k-joints. Note that a rigorous definition of k-joint and x-joint in terms of geometry and loading conditions is given in API (2014).

For members subject to combined axial compression and bending, the equations to satisfy are:

$$\frac{\sigma_a}{F_a} + \frac{C_m \sqrt{\sigma_{b,x}^2 + \sigma_{b,y}^2}}{1 - \frac{\sigma_a}{F_e'} F_b} \leq 1 \tag{2.62}$$

$$\frac{\sigma_a}{0.6 f_y} + \frac{\sqrt{\sigma_{b,x}^2 + \sigma_{b,y}^2}}{F_b} \leq 1 \tag{2.63}$$

where σ_a is the normal stress caused by axial force, F_a is the allowable axial compressive stress, f_y is the characteristic yield strength, $\sigma_{b,x}$ is the normal stress caused by bending about local x, $\sigma_{b,y}$ is the normal stress caused by bending about local y, F_a is the allowable axial compressive stress, F_b is the allowable bending stress, F_e' is the Euler stress divided by a safety factor per AISC 1989 and shown in Eq. (2.64), C_m is the reduction factor in the calculations of the utilization for members under compression and bending per API 2014 and shown in Eq. (2.65).

$$F_e' = \frac{12\pi^2 E}{23KLR} \tag{2.64}$$

$$C_m = 1 - 0.4\frac{\sigma_a}{F_e'} \tag{2.65}$$

The allowables are given by:

$$F_a = \frac{1 - \frac{KLR^2}{2C_c^2} f_y}{5/3 + \frac{3KLR}{8C_c} - \frac{KLR^3}{8C_c^3}} \quad \text{for } KLR < C_c \tag{2.66a}$$

$$F_a = \frac{12\pi^2 E}{23KLR^2} \quad \text{for } KLR \geq C_c \tag{2.66b}$$

$$\text{with} \quad C_c = \left(\frac{2\pi^2 E}{f_{y2}} \right)^{0.5} \tag{2.66c}$$

$$F_b = \begin{cases} 0.75 f_y & \text{for} \quad \frac{D}{t} \leq \frac{10{,}340\,\mathrm{N\,m^{-2}}}{f_y} \\ 0.84 - 1.74 \frac{f_y D}{Et} \; f_y & \text{for} \quad \frac{10{,}340\,\mathrm{N\,m^{-2}}}{f_y} < \frac{D}{t} \leq \frac{20{,}680\,\mathrm{N\,m^{-2}}}{f_y} \\ 0.72 - 0.58 \frac{f_y D}{Et} \; f_y & \text{for} \quad \frac{20{,}680\,\mathrm{N\,m^{-2}}}{f_y} < \frac{D}{t} \leq \frac{300\,\mathrm{N\,m^{-2}}}{f_y} \end{cases} \tag{2.66d}$$

where f_{y2} is the allowable used in local buckling axial stress determination per API 2014 given by:

$$f_{y2} = \min\left(f_{xc}, f_{xe}\right) \tag{2.67}$$

where the inelastic (f_{xc}) and elastic (f_{xe}) buckling stresses are given by:

$$f_{xc} = \begin{cases} f_y \left(1.64 - 0.23 \left(\frac{D}{t}\right)^{0.25}\right) & \text{for } \frac{D}{t} > 60 \\ f_y & \text{for } \frac{D}{t} \leq 60 \end{cases} \tag{2.68}$$

$$f_{xe} = 2C_{fxe} E \frac{t}{D} \tag{2.69}$$

where D is the generic member OD, C_{fxe} is the reduction factor in the calculation of the elastic buckling stress per API 2014, which is normally equal to 0.3.

For members under axial tension, the verification consists of the following inequality:

$$\sigma_a \leq 0.6 f_y \tag{2.70}$$

The left-hand sides of Eqs. (2.62)-(2.63) and Eq. (2.70) are used by JacketSE to directly output utilization values at all of the jacket members. The verification is conducted at all FEA nodes, and the stresses are calculated via basic mechanics starting from the loads obtained from the FEA solver—see Eq. (2.71):

$$\sigma_a = \frac{N_d}{A} \tag{2.71}$$

$$\sigma_b = \frac{M_d D}{2J_{xx}} \tag{2.72}$$

$$\tag{2.73}$$

where σ_b is normal stress caused by total bending moment.

Note that the jacket legs are assumed to be flooded, thus hydrostatic effects are ignored for the leg members. The mud- and cross-braces are sized through an engineering rule (see Sections 2.6 and 2.5) that grants sufficient strength over hydrostatic effects. In a future release of JacketSE, stresses due to hydrostatic pressure will be directly incorporated into the utilization calculations.

Joints are verified by considering loads from the intersecting members, denoted as the chord and brace. For a k-joint, the chord is the jacket leg; for an x-joint, the verification is repeated twice by having each of the two braces alternately play the role of the chord. The joint utilization is calculated via Eq. (2.74):

$$\frac{P_j}{P_a} + \left(\frac{M_j}{M_a} \right)_{IP}^2 + \left| \frac{M_j}{M_a} \right|_{OP} \leq 1 \tag{2.74}$$

Table 19. Values for c_1,c_2, and c_3 As a Function of Loading Conditions and Joint Type and $\beta_j = \frac{d_{jb}}{d_{jc}}$—From API (2014)

Joint type	c_1	c_2	c_3
k-joint under brace axial loading	0.2	0.2	0.3
x-joint under brace axial loading[a] $\beta_j \leq 0.9$	0.2	0	0.5
x-joint under brace axial loading[a] $\beta_j = 1$	-0.2	0	0.2

[a] Linear interpolation between β_j=0.9 and β_j=1.

where P_j is the brace axial load at the joint, P_a is the allowable capacity for brace axial load, M_j is the brace bending load at the joint, M_a is the allowable capacity for brace bending load, *IP* stands for in-plane, *OP* stands for out-of-plane.

The basic joint capacities are calculated as in Eq. (2.75):

$$P_a = Q_{ub} Q_{fc} \frac{f_{yc} t_{jc}^2}{\gamma_{j1} \sin\theta_j} \tag{2.75}$$

$$M_a = Q_{ub} Q_{fc} \frac{f_{yc} t_{jc}^2 d_{jb}}{\gamma_{j1} \sin\theta_j} \tag{2.76}$$

where Q_{ub} is the strength factor per API 2014, Q_f is the chord load factor per API 2014, f_{yc} is the chord allowable stress used in joint verification, t_{jc} is the chord thickness in a joint verification (also t_{leg}), θ_j is the smaller angle described by the brace's and chord's axes at the joint, γ_{j1} is the brace load PSF in a joint verification, which is normally set at 1.6.

Q_{fc} is calculated as in Eq. (2.77):

$$\begin{aligned} Q_{fc} = \;& 1 + c_1 \tfrac{P_c \gamma_{j2}}{P_{yc}} - c_2 \tfrac{M_{c,IP} \gamma_{j2}}{M_{pc}} - c_3 A_{jnt}^2 \\ \text{with } A_{jnt} = \;& \sqrt{\left(\tfrac{\gamma_{j2} P_c}{P_{yc}}\right)^2 + \left(\tfrac{\gamma_{j2} M_{c,IP}}{M_p}\right)^2} \end{aligned} \tag{2.77}$$

where c_1-c_3 are given in Table 19, P_c is the chord axial load at the joint, P_{yc} is the yield capacity of the chord at the joint, $M_{c,IP}$ is the chord *IP* bending load at the joint, M_{pc} is the plastic moment capacity of the chord at the joint, γ_{j2} is the chord PSF in a joint verification, which is normally set equal to 1.2. The average of the chord loads on either side of the brace intersection should be used in Eq. (2.77). The chord axial load is positive in tension, and chord *IP* bending is positive when it produces compression of the joint footprint.

The strength factor Q_{ub} is given by API (2014) as a function of brace loading type and joint type, as shown in Table 20. Note that, in Table 20, a gap factor Q_g is used, which is a function of the ratio between the adjacent brace distance at the k-joint with the leg (g_p) over the chord OD (d_{jc}), and of the ratios of brace-to-chord t's ($\frac{t_{jb}}{t_{jc}}$) and f_y's ($\frac{f_{yb}}{f_{yc}}$). In JacketSE the gap is calculated as:

$$g_p = \frac{d_{jc}}{2}\left(\tan\left(\frac{\pi}{2} - \alpha_{bl1}\right) + \tan\left(\frac{\pi}{2} - \alpha_{bl2}\right)\right) - \frac{D_{brc2}}{\sin(\alpha_{bl2})/2} - \frac{D_{brc1}}{\sin(\alpha_{bl1})/2} \tag{2.78}$$

where α_{bl1} and α_{bl2} are the angles between the braces and the leg, D_{brc1} and D_{brc2} are the braces's ODs at the k-joint under examination.

As shown in Eqs. (2.74) and (2.77), it is necessary to calculate the *IP* and *OP* components of the bending moments at the brace and chord. JacketSE performs a coordinate transformation from the FEA element local coordinate system to the triad that identifies the plane of the joint.

Table 20. Values for Q_{ub} As a Function of Brace Loading and Joint Type and $\beta_j = \frac{d_{jb}}{d_{jc}}$—From API (2014)

Joint type	brace load			
	axial tension	axial compression	*IP* bending	*OP* bending
k-joint	$\min\ 40\beta_j^{1.2}Q_g, (16+1.2\gamma_c)\beta_j^{1.2}Q_g$ [a],[b]		$(5+0.7\gamma_c)\beta_j^{1.2}$	$2.5+(4.5+0.2\gamma_c)\beta_j^{2.6}$
x-joint	$23\beta_j$ for $\beta_j \le 0.9$ $20.7+\ \beta_j-0.9\ \ (17\gamma_c-220)$ for $\beta_j > 0.9$	$2.8+(12+0.1\gamma_c)\beta_j\ \ Q_{beta}$ [c]		

[a] $Q_g = \begin{cases} \max\ 1, 1+0.2\ \ 1-2.8g_p/d_{jc}\ ^3 & \text{for } \frac{g_p}{d_{jc}} \ge 0.05 \\ 0.13+0.65\frac{t_{jb}f_{yb}}{t_{jc}f_{yc}}\sqrt{\gamma_c} & \text{for } \frac{g_p}{d_{jc}} \le -0.05 \\ \text{linear interpolation otherwise} \end{cases}$

[b] $\gamma_c = \frac{d_{jc}}{2t_{jc}}$

[c] $Q_{beta} = \begin{cases} \frac{0.3}{\beta_j(1-0.833\beta_j)} & \text{for } \beta_j > 0.6 \\ 1 & \text{for } \beta_j \le 0.6 \end{cases}$

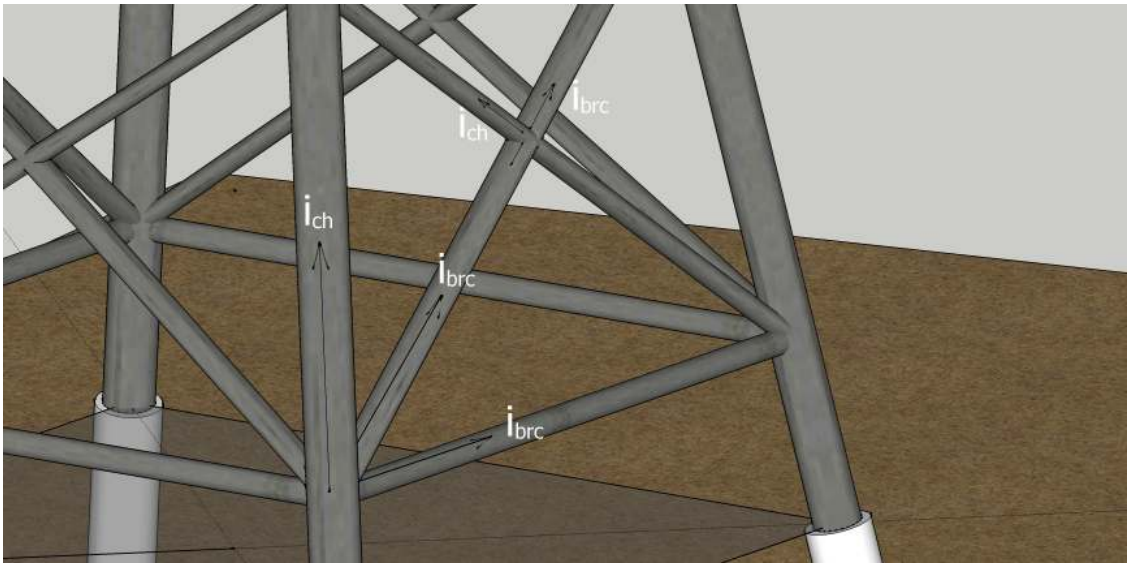

Figure 8. Typical unit vectors associated with x-joint and k-joint used in JacketSE to determine *IP* and *OP* bending moment components with respect to the joint plane

The generic *IP* and *OP* bending moment vectors are calculated via simple geometry rules as in Eq. (2.79).

$$\mathbf{M_{OP}} = \mathbf{M_{jnt}} \cdot \mathbf{C_{jnt,x}} \;\; \mathbf{C_{jnt,x}} + \mathbf{M_{jnt}} \cdot \mathbf{C_{jnt,y}} \;\; \mathbf{C_{jnt,y}} \tag{2.79}$$

$$\mathbf{M_{IP}} = \left[\begin{bmatrix} M_{jnt,x}\mathbf{C_{el,x}} \\ M_{jnt,y}\mathbf{C_{el,y}} \\ M_{jnt,z}\mathbf{C_{el,z}} \end{bmatrix} \cdot \mathbf{C_{jnt,z}} \right] \mathbf{C_{jnt,z}} \tag{2.80}$$

In Eq. (2.79), $\mathbf{M_{jnt}}$ is the bending moment vector for the generic member at the joint of interest, whose components are $M_{jnt,x}$-$M_{jnt,z}$ in the local FEA element coordinate system, $[\mathbf{C_{el}}]$ is the matrix identifying the local element coordinate system, i.e., the transformation from $\mathscr{F}\mathscr{F}_0$ to $\mathscr{F}\mathscr{F}_2$, with local x along the member axis and local y, z along the cross-section principal axes of inertia, which identifies the local FEA element coordinate system with respect to the global coordinate system, $\mathbf{C_{el,x}}$-$\mathbf{C_{el,z}}$ denote the three-element rows of $[\mathbf{C_{el}}]$, $[\mathbf{C_{jnt}}]$ is the direction cosine matrix identifying the joint plane, with x, y in the joint plane and z normal to it, with $\mathbf{C_{jnt,x}}$-$\mathbf{C_{jnt,z}}$ denoting its three-element rows (see Figure 8 and Eq. (2.81)):

$$[\mathbf{C_{jnt}}] = \begin{bmatrix} \mathbf{C_{jnt,x}} \\ \mathbf{C_{jnt,y}} \\ \mathbf{C_{jnt,z}} \end{bmatrix} = \begin{bmatrix} \hat{\mathbf{i}}_{\mathbf{ch}} \\ \hat{\mathbf{i}}_{\mathbf{ch}} \times \hat{\mathbf{i}}_{\mathbf{brc}} \quad \times \hat{\mathbf{i}}_{\mathbf{ch}} \\ \hat{\mathbf{i}}_{\mathbf{ch}} \times \hat{\mathbf{i}}_{\mathbf{brc}} \end{bmatrix} \tag{2.81}$$

where $\hat{\mathbf{i}}_{\mathbf{ch}}$ is the unit vector identifying the chord longitudinal axis, and $\hat{\mathbf{i}}_{\mathbf{brc}}$ is the unit vector identifying the x-brace longitudinal axis. The unit vectors are easily obtained from the coordinates of two adjacent nodes in the member of interest, which are also used to obtain $\delta_{\mathbf{el}}$, i.e., the distance vector between two adjacent nodes of a FEA element. $[\mathbf{C_{el}}]$ follows FRAME3DD's convention and is given by:

$$[\mathbf{C_{el}}] = [\mathbf{C}_\phi][\mathbf{C}_{\psi,\theta}] = \begin{bmatrix} \cos\psi_{el}\cos\theta_{el} & \cos\theta_{el}\sin\psi_{el} & -\sin\theta_{el} \\ \cos\psi_{el}\sin\phi_{el}\sin\theta_{el} - \sin\psi_{el}\cos\phi_{el} & \cos\phi_{el}\cos\psi_{el} + \sin\phi_{el}\sin\psi_{el}\sin\theta_{el} & \cos\theta_{el}\sin\phi_{el} \\ \cos\psi_{el}\cos\phi_{el}\sin\theta_{el} + \sin\psi_{el}\sin\phi_{el} & -\sin\phi_{el}\cos\psi_{el} + \cos\phi_{el}\sin\psi_{el}\sin\theta_{el} & \cos\theta_{el}\cos\phi_{el} \end{bmatrix} \tag{2.82}$$

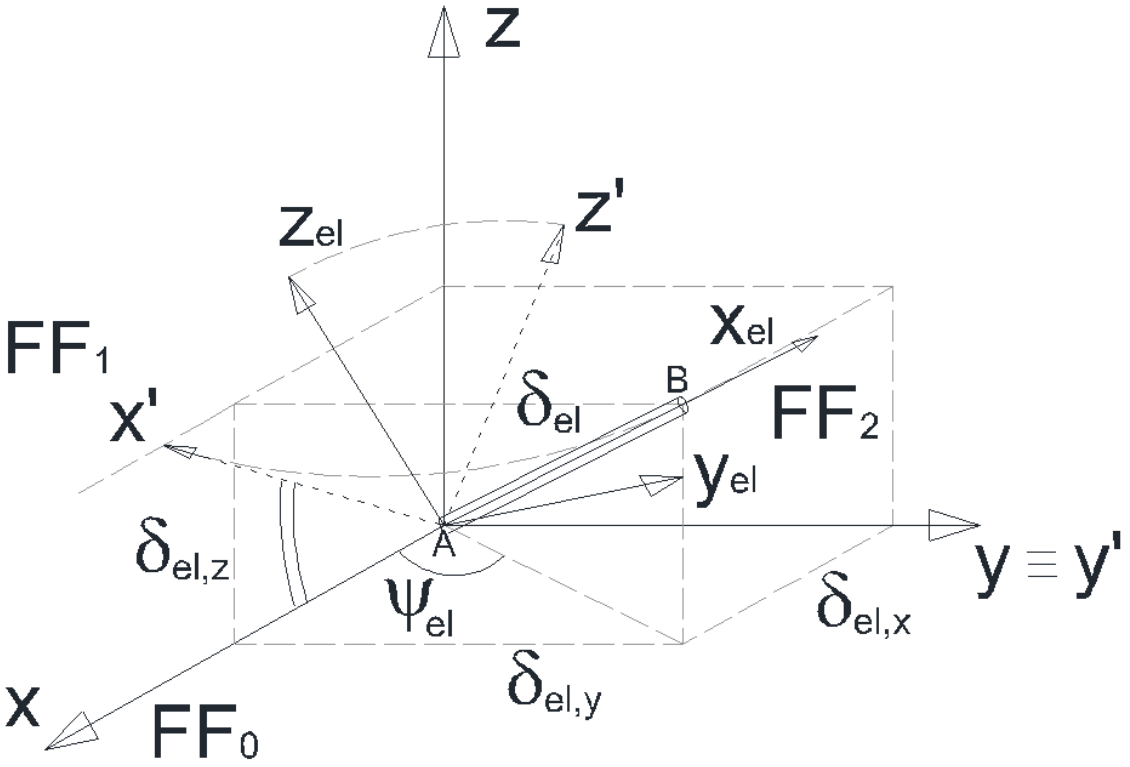

Figure 9. The element ($\mathscr{FF}_2$), intermediary ($\mathscr{FF}_1$), and global ($\mathscr{FF}_0$) coordinate system used in JacketSE. The generic element is shown as an $\overline{AB}$ cylindrical rod; the other symbols are explained in the text

with

$$[\mathbf{C}_{\psi,\theta}] = \begin{bmatrix} \cos\psi_{el}\cos\theta_{el} & \cos\theta_{el}\sin\psi_{el} & -\sin\theta_{el} \\ -\sin\psi_{el} & \cos\psi_{el} & 0 \\ \sin\theta_{el}\cos\psi_{el} & \sin\theta_{el}\sin\psi_{el} & \cos\theta_{el} \end{bmatrix} [\mathbf{C}_{\phi}] = \begin{bmatrix} 1 & 0 & 0 \\ 0 & \cos\phi_{el} & \sin\phi_{el} \\ 0 & -\sin\phi_{el} & \cos\phi_{el} \end{bmatrix} \tag{2.83}$$

where $[\mathbf{C}_{\psi,\theta}]$ is the matrix describing the transformation of coordinate systems from $\mathscr{FF}_0$ to $\mathscr{FF}_1$ via a rotation θ_{el} about the global y and a rotation ψ_{el} about global z, θ_{el} is the rotational angle about the global y (per FRAME3DD's convention) (see also Figure 9 for the definition of the $\mathscr{FF}_0$, $\mathscr{FF}_1$, and $\mathscr{FF}_2$ coordinate systems), ψ_{el} is the rotational angle about the global z (per FRAME3DD's convention), $[\mathbf{C}_{\phi}]$ is the matrix describing the transformation of coordinate systems from $\mathscr{FF}_1$ to $\mathscr{FF}_2$ via a rotation about the local x, and ϕ_{el} is the eulerian rotational angle about the local x, which is taken as 0 rad for tubular members. θ_{el} and ψ_{el} are calculated as in Eqs. (2.84)-(2.85):

$$\psi_{el} = \arctan\frac{\delta_{el,y}}{\delta_{el,x}} \tag{2.84}$$

$$\theta_{el} = \arctan\frac{\delta_{el,z}}{\sqrt{\delta_{el,x}^2 + \delta_{el,y}^2}} \tag{2.85}$$

where $\delta_{el,x}$-$\delta_{el,z}$ are the components of the distance vector $\boldsymbol{\delta}_{\mathbf{el}}$, see also Figure 9.

Finally, because API (2014) permits a 33% increase of the given allowables, JacketSE includes a $\frac{4}{3}$ factor in all of the allowables shown above for the jacket utilization.

3 Preliminary Verification and Validation

Damiani and Song (2013) show a comparison of the results in terms of modal and static loads analyses performed by JacketSE and ANSYS for a few representative jacket-tower configurations. ANSYS models utilized second-order beam and pipe elements but also shell elements for the TP. The results showed little dependence on the number of elements used.

Two figures from Damiani and Song (2013) are reproduced in Figure 10. Figure 10a shows the first eigenmode for a structure supporting a 10 MW OWT as calculated by ANSYS. The associated frequency (0.2132 Hz shown in the graph) matched the JacketSE-calculated one of 0.21 Hz rather well. Figure 10b shows the von-Mises stress distribution in the jacket. The maximum pile and leg axial forces were within 5% of those calculated by JacketSE's pyFrame3DD, thus lending credibility to the loads and utilization calculation. For more details on these and more results and verification against ANSYS, see Damiani and Song (2013).

Damiani et al. (2016) examines the effect of varying turbine ratings, hub heights, water depths, waves, and tower-top masses on the structural overall support mass for OWTs. The primary motivation of that research lay in determining key relationships between environmental design drivers and costs associated with wind plant BOS, as well as with the operation and maintenance.

The results obtained by running optimizations of jacket-tower configurations were compared to data available from industry experience. Data from actual installations and other studies (GL Garrad Hassan 2012; BVG Associates 2012) that have predictions on steel quantities are plotted in the graphs of Figure 11. In that figure, the surface that best fits the model-devised data was extrapolated towards lower hub heights to compare to the industry data. As shown, the results of the model, extrapolated toward lower hub heights and water depths, agree relatively well with the industry data for water depths between 20 m and 40 m, but underestimate and overestimate the mass for shallower and deeper depths, respectively. This may be because of the coarse resolution in the data considered, which did not include any points in the depth range between 45 m and 55 m and below 20 m. The gradient of the jacket mass with respect to water depth above 40 m and below 10 m may therefore be artificially overestimated.

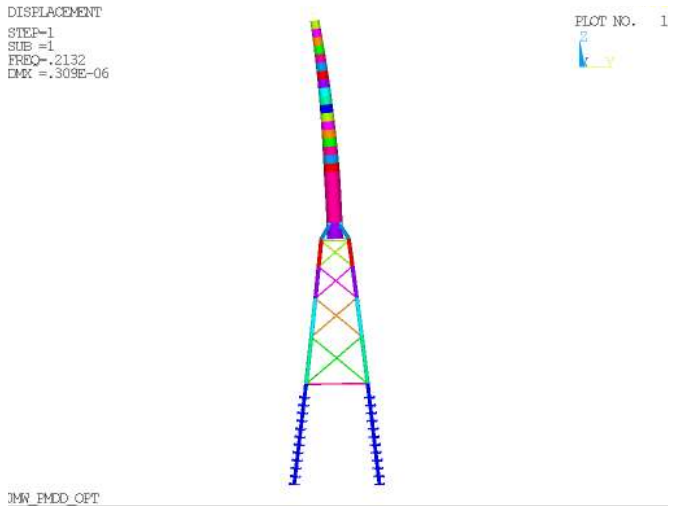

(a)

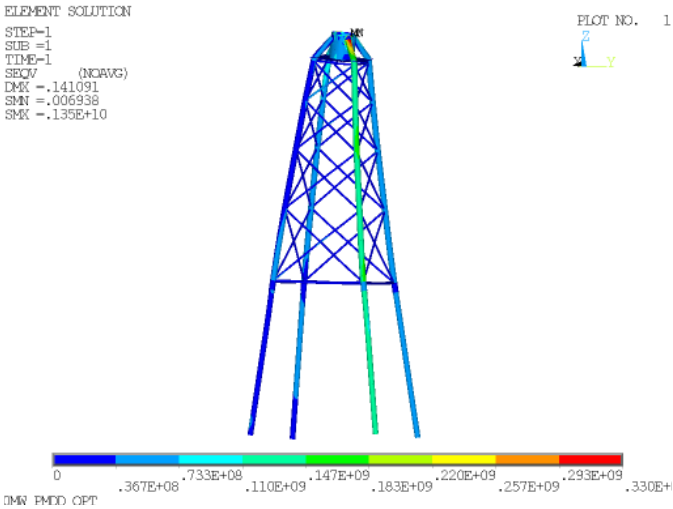

(b)

Figure 10. Results from the ANSYS analysis of a jacket-tower-pile configuration for a 10 MW OWT; (a) shows the first eigenmode; (b) shows the von-Mises stress distribution in the jacket members. From Damiani and Song (2013)

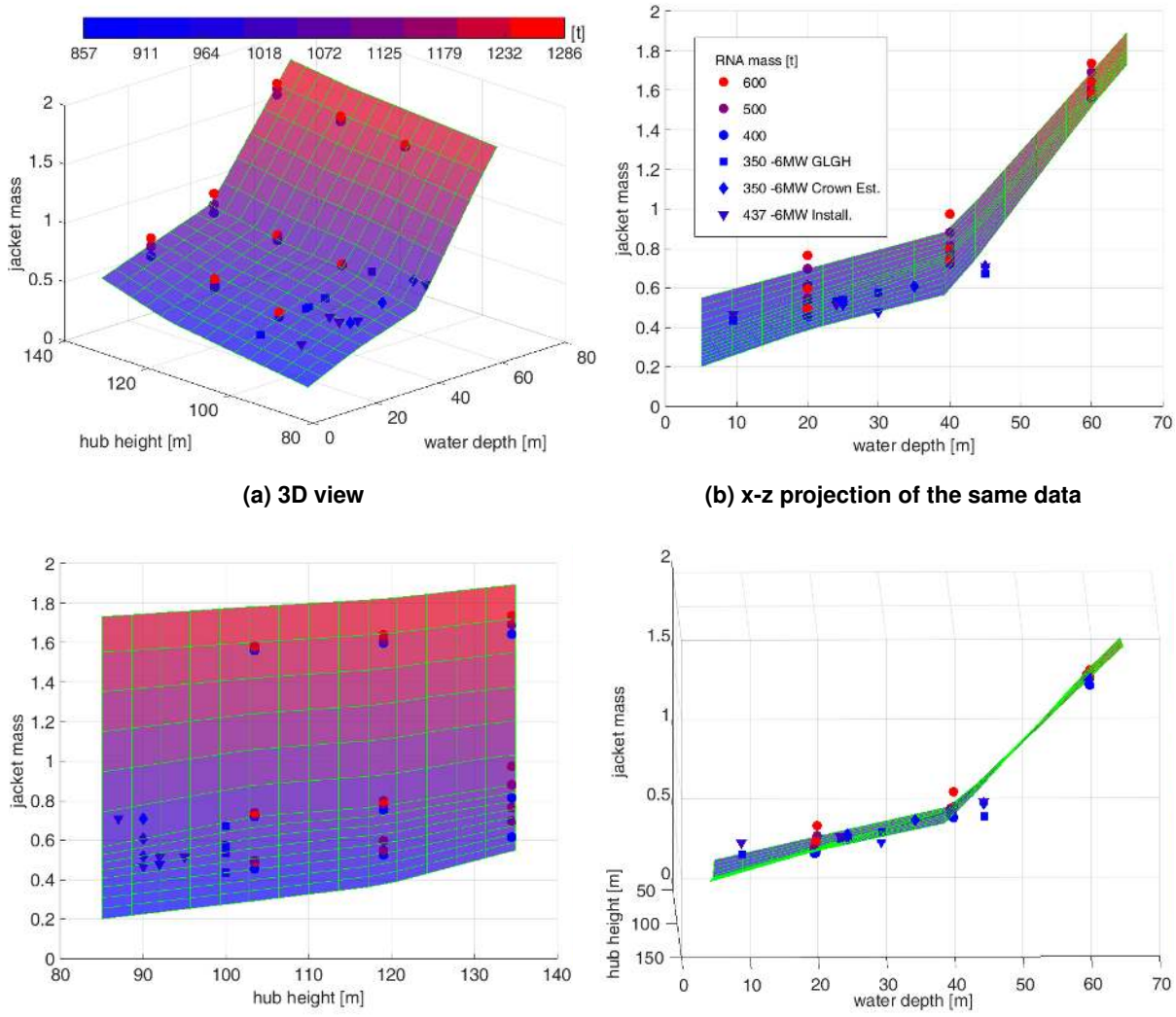

(a) 3D view

(b) x-z projection of the same data

(c) y-z projection of the same data

(d) Same data, but oriented to show the distance of data points from best fit curve

Figure 11. Jacket steel mass trend for 6 MW turbine configurations. The study 81 data points are denoted by filled circles, with colors indicating RNA mass as denoted by the legend in (b). The surface (bilinear interpolation of the data points) is color-coded by jacket mass tonnage, and the legend is given in (a). In all the plots, the z-axis shows jacket mass made non-dimensional with its average across all the 6 MW cases. Other symbols indicate: existing installations of 6 MW offshore turbines (triangles); predictions from the Crown Estate study BVG Associates 2012 (diamonds); and predictions from GL Garrad Hassan 2012 (squares). From Damiani et al. (2016)

4 Case Study

A simple case was set up to show the capabilities of JacketSE. A 6 MW turbine was imagined installed at a site with a 40.8 m water depth. The main loads from the RNA and turbine parameters are given in Table 21, whereas environmental parameters are shown in Table 22. The soil was assumed to be sand with stratigraphy as per Table 3. Piles were considered unplugged. ASTM-992 steel was considered for all components (ASTM 2015), but its density was taken as 8500 $\mathrm{kg\,m^{-3}}$.

An optimization scheme that makes use of SNOPT—Sparse Nonlinear OPTimizer, a software package for solving large-scale optimization problems (Gill, Murray, and Saunders 2005)—was implemented. The objective was set to minimize the total structural mass. Bounds for the design variables are given in Table 23. Note that the tower top OD was fixed at 3.51 m to match a given nacelle yaw bearing size. The jacket was assumed to be of the prepile type with vertical piles, and a TP lumped mass of 75 t (metric tonnes) was also included. Five bays were selected based on past experience with similar designs.

The initial-guess configuration did not meet either the pile capacity constraint or the eigenfrequency target, but met utilization constraints. Results of the optimization are shown in Figures 12 and 13, and Table 24. Figure 12 shows the stick diagram of the resulting jacket-tower configuration; Figure 13 shows the outline of the tower and the calculated utilization values along the span for the two DLCs. It can be seen from the graph in Figure 13, that the local buckling criteria drove the tower design. In general, the operational conditions dominated the design when compared to the parked DLC. Maximum utilization was seen just above the mid-height of the tower.

The obtained values for the design variables and the component mass schedule are given in Table 24, where they can also be compared to the initial guess values. The batter did not change significantly, and, as a result, neither did the footprint. The tower and TP mass decreased with respect to the starting configuration, whereas the piles' and the main lattice's mass increased. This increment in mass was necessary to keep the first eigenfrequency within the selected tolerance and to ensure the pile capacity constraint was satisfied, and only caused some 1% penalty on the overall mass.

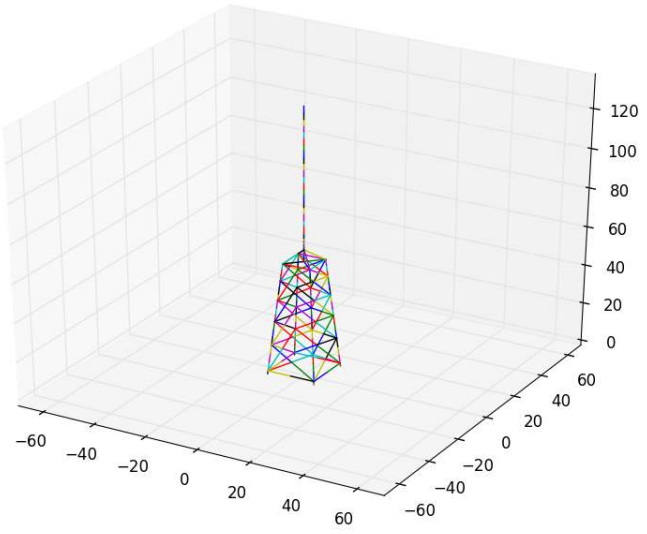

Figure 12. Diagram of the jacket-tower configuration as calculated by the optimizer for this case study

Table 21. Turbine and Substructure Parameters for the Case Study

Parameter	Unit	Value	Comments
Generator rating	MW	6	
z_{hub}	m MSL	97	From project data
z_{dbot}	m MSL	16	From project data
n_{bays}	-	5	Based on experience
TP lumped mass	t (metric tonne)	75	
RNA mass	t	365	
RNA $[I_{xx}, I_{yy}, I_{zz}]$	kg m^2	$[7.92E7, 4.26E7, 4.04E7]$	
RNA $[I_{xy}, I_{xz}, I_{yz}]$	kg m^2	$[2.39E2, 1.78E6, 2]$	
RNA $\mathbf{CM_{off}}$	m	$[-4.1, 0, 3.04]$	
DLC 1.6 $\mathbf{F_{aero}}$	N	$[1.94E6, -2.12E5, -1.46E5]$	Max thrust case
DLC 1.6 $\mathbf{M_{aero}}$	N m	$[5.35E6, 1.56E7, -1.8E6]$	"
DLC 6.1 $\mathbf{F_{aero}}$	N	$[1.80E5, -4.21E4, 1.28E5]$	Max wind gust case
DLC 6.1 $\mathbf{M_{aero}}$	N m	$[-1.42E4, 1.11E7, -1.39E5]$	"
RNA $\delta_{\mathbf{thoff}}$	m	$[-7.76, 0, 3.5]$	
Target eigenfrequency	Hz	0.28	

Table 22. Environmental Parameters Used for the Case Study

Parameter	Unit	Value	Comments
Water depth	m	40.8	Long Island (US)
50 yr wave height	m	17.6	From NOAA buoy data
50 yr wave period	s	12.5	From NOAA buoy data
50 yr gust speed	m s^{-1}	55	From actual project
Max-thrust wind speed	m s^{-1}	20	From actual project

Table 23. Key Constraints Used in This Study for the Sizing Tool

Parameters	Units	Values
Pile OD min-max	m	0.8-2.5
Pile t min-max	m	0.0381-0.0762
Max embedment length	m	60
Max footprint	m	23
Leg OD min-max	m	0.8-3
Leg t min-max	m	0.0318-0.0635
X-brace OD min-max	m	0.32-2.4
X-brace t min-max	m	0.0191-0.0508
Mud-brace OD min-max	m	0.32-2.4
Mud-brace t min-max	m	0.0318-0.0508
Brace OD/Leg OD	-	0.3
Brace DTR	-	≥ 31 AND ≤ 50
Brace buckling-parameter KLR^c	-	$\leq 70.$
Girder OD min-max	m	0.8-1.3
Girder t min-max	m	0.0127-0.0635
Deck width/Tower-base OD min-max	m	2-2.1
Tower-base OD min-max	m	4-6
Tower-top OD min-max	m	3.51 (fixed)
Tower DTR	-	120-250
Tower waist/tower length max	-	0.25
First eigenfrequency acceptable band above target	%	5

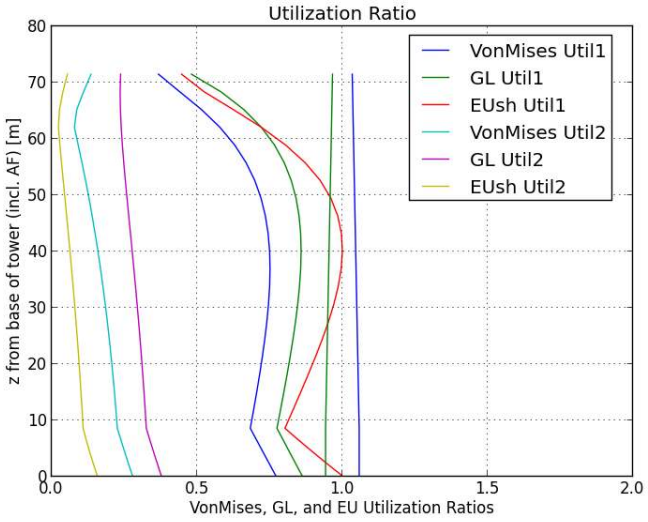

Figure 13. Calculated tower utilizations for the mass-optimized jacket-tower configuration used in this case study. VonMises Util1 and Util2 refer to utilizations with respect to yield strength, GL Util1 and Util2 refer to global (Eulerian) buckling criteria, and EUsh Util1 and Util2 refer to the shell buckling criteria. GL and EUsh Util1's refer to the first DLC, while GL and EUsh Util2's refer to the second

Table 24. Values of the Design Variables for the Calculated Minimum Mass Configuration

Parameters	Units	Initial Guess	Optimized Values
Pile OD	m	1.2	1.61
Pile *t*	m	0.04	0.0381
Embedment length	m	60	60
Piles' mass	t	297	385
Batter	-	15	14.87
Footprint	m	18.22	18
Leg OD	m	0.9	0.98
Leg *t*	m	0.04	0.0318
X-brace OD	m	0.6	0.59
X-brace *t*	m	0.02	0.0191
Mud-brace OD	m	0.8	0.98
Mud-brace *t*	m	0.04	0.0318
Lattice mass	t	509	467
Deck width	m	12.6	11.94
Girder OD	m	0.9	1.08
Girder *t*	m	0.04	0.03
Strut OD	m	0.9	0.98
Strut *t*	m	0.04	0.0318
Diagonal brace OD	m	0.9	1.08
Diagonal brace *t*	m	0.04	0.03
Shell OD	m	6	5.97
Shell *t*	m	0.04	0.048
TP length	m	6	6
TP mass	t	206	198
Tower-base OD	m	6	5.97
Tower-base *t*	m	0.03	0.0323
Tower-top OD	m	3.51	3.51 (fixed)
Tower length	m	71.5	71.5 (fixed)
Tower waist height	m	17.5	8.6
Tower mass	t	263	243
Total mass	t	1276	1293
First and second eigenfrequencies	Hz	0.3,0.31	0.29, 0.296

5 Conclusions and Future Work

The support structure plays an important role in defining the OWT system reliability and performance characteristics, but it is also the primary driver in the BOS costs. Suboptimal designs of the support structure are particularly detrimental because they directly influence CapEx and the O&M costs. Important trade-offs in the design of an OWT subsystems could be easily missed by the industry practice, uncoupled design-process, in which each component is designed independently. The system cost resulting from such an approach can be higher than that of the optimal solution. In contrast, an integrated design of the turbine and support structure might significantly lower the overall system cost. To enable this system-level optimization, we developed JacketSE, a CAE tool within NREL's systems engineering WISDEM toolbox, which connects physics-based models of all major system components, and allows engineers and designers to explicitly capture the trade-offs between their designs. JacketSE leads to configurations of towers, jackets, and piles for given environmental conditions and turbine parameters.

JacketSE is based on a simplified treatment of the physics, namely simplified hydrodynamics and material mechanics. The main modules were described together with the math and standards equations used for the sizing, load calculations, and member utilization calculations. Preliminary verification against the commercial package ANSYS showed good accuracy in the modal and static loads analyses performed by the FEA solver in JacketSE.

A case study was run to show the capabilities when coupled with an optimization algorithm seeking minimum overall mass. Only a couple of design driving load cases were considered for the optimization cycle, but results have proven encouraging when compared to industry data in other studies (Damiani et al. 2016).

JacketSE can be used to evaluate LCOE trends as functions of main parameters and to assess CapEx and LCOE sensitivity to: project characteristics (size and turbine spacing), technology (turbine size, substructure and foundation type, electrical infrastructure), and geospatial properties (water depth and distance to shore).

Future research will enhance and validate the model capabilities, including revised FEA, hydrodynamics, fatigue, and soil-pile interaction.

Bibliography

ABS. 2014. *Guide for BUCKLING AND ULTIMATE STRENGTH ASSESSMENT FOR OFFSHORE STRUCTURES*. American Bureau of Shipping, ABS Plaza, 16855 Northchase Drive, Houston, TX 77060 USA.

AISC. 1989. *AISC 335:1989 - Specification For Structural Steel Buildings - Allowable Stress Design, Plastic Design*. Superseded by AISC 360-10. AISC, American Institute of Steel Construction, One East Wacker Drive, Suite 700-Chicago, Illinois 60601-1802.

ANSI. 2010. *Specification for Structural Steel Buildings*. 3rd printing: 2013. ANSI/AISC, American Institute of Steel Construction, One East Wacker Drive, Suite 700-Chicago, Illinois 60601-1802.

API. 2014. *Planning, Designing and Constructing Fixed Offshore Platforms - Working Stress Design*. API RECOMMENDED PRACTICE 2A-WSD. American Petroleum Institute, API Publishing Services, 1220 L Street, NW, Washington, DC 20005.

ASTM. 2015. *ASTM A992 / A992M - 11(2015) Standard Specification for Structural Steel Shapes*. ASTM, West Conshohocken, PA. www.astm.org.

AWEA. 2012. *Offshore Compliance Recommended Practices Ű Recommended Practices for Design, Deployment and Operation of Offshore Wind Turbines in the United States*. AWEA.

Bowles, J. E. 1997. *Foundation Analysis and Design*. 5th. 1168 pp. The McGraw-Hill Companies, Inc.

Burton, T., et al. 2005. *Wind Energy Handbook*. 1st. 617. 111 River St., Hoboken, NJ 07030, USA: John Wiley / Sons, Inc.

BVG Associates. 2012. *Offshore wind cost reduction pathways Ű technology work stream*. Technical Report. The Crown Estate.

Chakrabarti, S. K. 1987. *Hydrodynamics of Offhore Structures*. 440 p. Southampton, UK: WIT Press.

– , ed. 2005. *Handbook of Offshore Engineering*. 2 volume set –1321 pp. The Boulevard Langford Lane, Kidlington, Oxford OX5 lGB, UK: Elsevier.

Cordle, A., G. McCann, and W. de Vries. 2011. "Design drivers for offshore wind turbine jacket support structures". In *ASME 2011 30th International Conference on Ocean, Offshore and Arctic Engineering- OMAE2011*, 419–428. Rotterdam, THe Netherlands: ASME.

Damiani, R. 2016. "Offshore WInd Turbine Design". Chap. 8—Offshore Wind Turbine Tower Design, ed. by Elsevier. In Press. Elsevier.

Damiani, R., and H. Song. 2013. "A Jacket Sizing Tool for Offshore Wind Turbines Within the Systems Engineering Initiative". In *Offshore Technology Conference*. Houston, Texas, USA: Offshore Technology Conference. doi:http://dx.doi.org/10.4043/24140-MS.

Damiani, R., et al. 2016. "Scenario Analysis For Techno-Economic Model Development of U.S. Offshore Wind Support Structures". In review, *Wind Energy*.

De Vries et al. 2011. *Final Report WP4.2: Support Structure Concepts for Deep Water Sites*. Technical Report UpWind_WP4_D4.2.8_Final Report. Project Upwind Contract No. 019945 (SES6).

DIN. 2005. *DIN 1055-4 (2005-03): Action on Structures - Part 4: Wind Loads*. Deutsches Institut Fur Normung E.V.

DNV. 2010. *Offshore Standard DNV-OS-C501 - Composite Components*. Det Norske Veritas AS, Veritasveien 1 - N-1322 HØVIK,Norway.

DNV. 2013. *Design of Offshore Wind Turbine Structures*. Offshore Standard. DNV, DET NORSKE VERITAS AS.

Dykes, K., et al. 2011. *Applications of Systems Engineering to the Research, Design, and Development of Wind Energy Systems*. Technical Report TP-5000-52616. Contract No. DE-AC36-08GO28308. 1617 Cole Boulevard, Golden, Colorado: NREL.

European Committee for Standardisation. 1993. *Eurocode 3: Design of Steel Structures—Part 1-6: General rules—Supplementary rules for the shell structures*. European Committee for Standardisation.

– . 2005. *Eurocode 3: Design of Steel Structures—Part 1-1: GenStructures and rules for buildings*. European Committee for Standardisation.

– . 2010. *Eurocode 1: Actions on Structures—Part 1-4: General actions—Wind actions*. European Committee for Standardisation.

EWEA. 2015. *The European offshore wind industry - key trends and statistics 2014*. Tech. rep. European Wind Energy Association.

Gavin, H. P. 2010. "User Manual and Reference for Frame3DD: A Structural Frame Analysis Program" [**inlang**C++]. Duke University. https://nees.org/resources/1650/download/frame3dd.pdf.

Germanischer Lloyd. 2005. *Guideline for the Certification of Offshore Wind Turbines*. Germanischer Lloyd, Germanischer Lloyd.

– . 2012. *Guideline for the Certification of Offshore Wind Turbines*. Germanischer Lloyd, Germanischer Lloyd.

Gill, P. E., W. Murray, and M. A. Saunders. 2005. "SNOPT: An SQP Algorithm for Large-Scale Constrained Optimization". *SIAM REVIEW* 47 (1): 99–131. doi:10.1137/S0036144504446096.

GL Garrad Hassan. 2012. "Expected Offshore Wind Farm balance of Station Costs in the United States". NREL's Subcontractor's report.

IEC. 2005. *61400-1. Wind turbines - Part 1: Design requirements*. International Electrotechnical Commission, IEC TC-88.

– . 2009. *61400-3 Wind turbines - Part 3: Design requirements for offshore wind turbines*. International Electrotechnical Commission, IEC TC-88.

ISO. 2007. *19902:2007 - Petroleum and natural gas industries – Fixed steel offshore structures*. ISO, ISO, ISO copyright office, Case postale 56, CH-1211 Geneva 20, Switzerland.

– . 2014. *19901-1:2005 (Modified) - Petroleum and natural gas industries – Specific requirements for offshore structures – Part 1: Metocean Design and Operating Considerations*. ANSI/API Recommended Practice 2MET. ISO, ISO, ISO copyright office, Case postale 56, CH-1211 Geneva 20, Switzerland.

Matlock, H., and L. C. Reese. 1960. "Generalized solutions for laterally loaded piles." *J. Soil Mechanics & Foundation Division* 86 (5): 91–97.

Molde, H., D. Zwick, and M. Muskulus. 2014. "Simulation-based optimization of lattice support structures for offshore wind energy converters with the simultaneous perturbation algorithm". *Journal of Physics: Conference Series* 555 (012075). doi:doi:10.1088/1742-6596/555/1/012110.

Mone, C., et al. 2015. *Cost of Wind Energy Review*. Technical Report TP-5000-63267. Golden, CO: NREL.

Murtagh, P. J., B. Basu, and B. M. Broderick. 2007. "Gust Response Factor Methodology for Wind Turbine Tower Assemblies". *J. of Structural Engineering* 133 (1): 139–144. doi:http://dx.doi.org/10.1061/(ASCE)0733-9445(2007)133:1(139).

Murthy, V.N.S. 2002. *Geotechnical Engineering - Principles and Practices of Soil Mechanics and Foundation Engineering*. Civil and Environmental Engineering. 1056 pp. 270 Madison Ave., New York, NY 10016: Marcel Dekker, Inc.

Musial, W. D., S. Butterfield, and B. Ram. 2006. "Energy from Offshore Wind". In *Offshore Technology Conference*. Houston, TX.

NREL. 2015. *WISDEM - The Wind-Plant Integrated System Design and Engineering Model set*. Accessed on November 4, 2015; https://github.com/WISDEM.

Panzer, H., et al. 2009. *Generating a Parametric Finite Element Model of a 3D Cantilever Timoshenko Beam Using Matlab*. Technical Reports on Automatic Control TRAC-4. Technische Universitat Munchen.

Pender, M. J. 1993. "Aseismic Pile Foundation Design Analysis". *Bullettin of the New Zealand National Society for Earthquake Engineering* 26 (1): 49–159.

Randolph, M. F. 1981. "Pile subject to torsion". *J. Geotech. Engrg. Div.* 107:1095–1111.

SEI. 2005. *Minimum Design Loads for buildings and other structures*. 388 pp. ASCE Standard, ASCE/SEI 7-05. American Society of Civil Engineers.

– . 2010. *Minimum Design Loads for buildings and other structures (ASCE/SEI 7-10)*. 3rd printing. 388 pp. ASCE Standard, ASCE/SEI 7-10. 1801 Alexander Bell Drive, Reston, Virginia 20191: American Society of Civil Engineers.

Timoshenko, S. 1970. *Theory of elasticity*. 3rd. Engineering societies monographs. 567 pp. McGraw-Hill Kogakusha Ltd.

Zwick, D., et al. 2014. "Comparison of different approaches to load calculation for the OWEC Quattropod jacket support structure". *Journal of Physics: Conference Series* 555 (012110). doi:doi:10.1088/1742-6596/555/1/012110.